

Protic NHC iridium complexes with β -H reactivity – synthesis, acetonitrile insertion, and oxidative self-activation

Mark K. Rong,[†] Andrei Chirila,[†] David Franciolus,[†] Martin Lutz,[‡] Martin Nieger,[§] Andreas W. Ehlers,^{†,||,⊥} J. Chris Slootweg^{*,†,⊥} and Koop Lammertsma^{*,†,||}

[†] Department of Chemistry and Pharmaceutical Sciences, VU University Amsterdam, De Boelelaan 1083, 1081 HV Amsterdam, The Netherlands.

[‡] Crystal and Structural Chemistry, Bijvoet Center for Biomolecular Research, Utrecht University, Padualaan 8, 3584 CH Utrecht, The Netherlands.

[§] Department of Chemistry, University of Helsinki, A. I. Virtasen aukio 1, P.O. Box 55, Helsinki, Finland.

^{||} Department of Chemistry, Oakland Park 2006, University of Johannesburg, Johannesburg, South Africa.

[⊥] Current address: Van 't Hoff Institute for Molecular Sciences, University of Amsterdam, Science Park 904, 1098 XH Amsterdam, The Netherlands.

SUPPORTING INFORMATION

TABLE OF CONTENTS

1. Experimental Details	S2
2. NMR-spectra	S5
3. Crystal structure determinations	S21
4. Optimized Structures	S24

1. Experimental Details

General considerations

All experiments were performed under an atmosphere of dry nitrogen using standard Schlenk-line and glovebox techniques, unless stated otherwise. Solvents were distilled under nitrogen over the appropriate drying agent; CaCl₂ (DCM), benzophenone/NaK (Et₂O, THF), LiAlH₄ (pentane), K₂CO₃ (MeCN, acetone), P₂O₅ (CD₂Cl₂, CDCl₃). C₆D₆ was dried over Na at room temperature. Anhydrous MeOH was obtained from Sigma-Aldrich. Water was degassed ultrasonically under reduced pressure. 2-Azido-phenyl isonitrile (**1**)¹ was kindly provided by C. A. Dumke and F. E. Hahn.² All other reagents were used as received. Solids were predried *in vacuo* for at least 15 min. NMR spectra were recorded on Bruker Avance 400 (¹H, 400.13 MHz; ¹³C{¹H}, 100.61 MHz, room temperature) or a Bruker Avance 500 (¹H, 500.23 MHz; ¹³C{¹H}, 125.78 MHz; room temperature). Chemical shifts are reported in ppm downfield from tetramethylsilane. ¹H-spectra were internally referenced to residual solvent resonances: CDCl₃ (δ 7.26) and CD₂Cl₂ (δ 5.32). ¹³C-spectra were internally referenced to residual solvent resonances: CDCl₃ (δ 77.16) and CD₂Cl₂ (δ 53.84). Melting points were measured using a Büchi Melting Point M-565 (sealed capillaries) and are uncorrected. High resolution electrospray ionization (ESI) mass spectrometry was carried out using a Bruker micrOTOF-Q instrument in positive ion mode (capillary potential of 4500 V). Infrared spectra have been recorded on a Shimadzu FT-IR 8400S spectrophotometer.

(1,2,3,4,5-pentamethylcyclopentadienyl) iridium(III) dichloride dimer³

Prepared according to literature procedures.

1,3-dimethyl-benzimidazolium iodide⁴

Prepared according to literature procedures.

Bis(1,3-dimethylbenzimidazolidin-2-ylidene)⁵

Prepared according to literature procedures.

(2-azidophenylisonitrile) (1-methyl-4-isopropyl-benzene) ruthenium(II) dichloride⁶

Prepared according to literature procedures.

(2-azidophenylisonitrile) (1,2,3,4,5-pentamethylcyclopentadienyl) rhodium(III) dichloride

[RhCp*Cl₂] (94 mg, 0.15 mmol, 1.0 eq.) in DCM (15 mL) was added to 2-azidophenylisonitrile (49 mg, 0.34 mmol, 2.3 eq.) to provide a red solution, which was stirred for 43.5h at RT, in absence of light. Evaporation provided a red powder, which was washed with Et₂O (3 x 10 mL) to provide [RhCp*(2-azidophenyl isonitrile)Cl₂] as a red powder (107 mg, 0.24 mmol, 77.7%). [RhCp*(2-azidophenyl isonitrile)Cl₂] was stored as a solid in absence of light at -20 °C. Mp: 324 °C ≤ decomp. ¹H NMR (500.23 MHz, CD₂Cl₂): δ = 7.54-7.47 (m, 2H, *o,m*-Ar-*H*), 7.31 (d, ³J_{H,H} = 8.5 Hz, 1H, *m*-Ar-*H*), 7.21 (t, ³J_{H,H} = 7.6 Hz, 1H, *p*-Ar-*H*), 1.81 (s, 15H, Cp*-CH₃). ¹³C{¹H}-NMR (125.78 MHz, CD₂Cl₂): δ = 138.0 (s, *m*-Ar-C-N₃), 131.7 (s, *o*-Ar-CH), 128.8 (s, *m*-Ar-CH), 125.8 (s, *m*-Ar-CH), 119.5 (s, *p*-Ar-CH), 101.1 (s, Cp*-CCH₃), 9.7 (s, Cp*-CCH₃), signals for Ar-CNC and Ar-CNC are unresolved. FT-IR: ν = 3086 (w), 3013 (w), 3003 (w), 2966 (w), 2947 (w), 2918 (w), 2897 (w), 2353 (w), 2289 (w), 2176 (s), 2141 (s), 2125 (s), 2050 (w), 2029 (w), 1992 (w), 1979 (w), 1967 (w), 1952 (w), 1578 (w), 1560 (w), 1489 (s), 1472 (m), 1445 (m), 1406 (w), 1375 (w), 1358 (w), 1310 (s), 1292 (m), 1263 (w), 1219 (w), 1204 (w), 1148

¹ Hahn, F.E.; Langenhahn, V.; Meier, N.; Lügger, T.; Fehlhammer, W.P. *Chem. Eur. J.*, **2003**, *9*, 704–712.

² Institut für Anorganische und Analytische Chemie, WWU Münster, Corrensstr. 28/30, D-48149 Münster, Germany.

³ R.G. Ball, W.A.G. Graham, D.M. Heinekey, J.K. Hoyano, A.D. McMaster, B.M. Mattson, S.T. Michel, *Inorg. Chem.*, **1990**, *29*, 2023–2025.

⁴ B. Bostai, Z. Novák, A.C. Bényei, A. Kotschy, *Org. Lett.* **2007**, *9*, 3437–3439.

⁵ E. Çetinkaya, P.B. Hitchcock, H. Küçükbay, M.F. Lappert, S. Al-Juaid, *J. Organomet. Chem.*, **1994**, *481*, 89–95.

⁶ O. Kaufhold, A. Flores-Figueroa, T. Pape, F.E. Hahn, *Organometallics*, **2009**, *28*, 896–901.

(m), 1092 (m), 1080 (m), 1040 (m), 1018 (m), 966 (w), 906 (w), 825 (w), 781 (s), 733 (m), 648 (m), 621 (w), 565 (m), 546 (m), 530 (m), 511 (w), 484 (w), 440 (w) cm^{-1} . HRMS (ESI-Q-TOF): calcd for $\text{C}_{17}\text{H}_{19}\text{ClIrRh}$: 417.0348; found 417.0366.

(1H-benzimidazolylidene) (1,2,3,4,5-pentamethylcyclopentadienyl) iridium(III) diiodide (4)

Alternative protocol 1: FeCl_3 (27 mg, 0.165 mmol, 1.5 eq.) was dissolved in acetonitrile (12 mL), after which NaI (150 mg, 1 mmol, 9.1 eq.) was added to provide a black suspension. Immediately afterwards, a solution of [(2-azidophenylisonitrile)IrCp*Cl₂] (60 mg, 0.11 mmol, 1.0 eq.) in DCM (3 mL) was added to the black suspension and the resulting mixture was stirred for 4h at RT. Volatiles (including iodine) were removed *in vacuo* to provide a black residue, which was extracted in DCM (40 mL) under atmospheric conditions. The dark extract was subsequently washed with a solution of $\text{Na}_2\text{S}_2\text{O}_3$ (100 mL, 20% in H_2O) and NaHCO_3 (100 mL, saturated solution in H_2O). The resulting orange solution was dried over Na_2SO_4 . After evaporation, [(1H-benzimidazolylidene)IrCp*I₂] was obtained as a dark yellow powder (48 mg, 0.07 mmol, 63%).

Halogen exchange: When a mixture of [(1H-benzimidazolylidene)IrCp*I₂] and [(1H-benzimidazolylidene)IrCp*ICl] was obtained, the obtained mixture was dissolved in acetone (66 mL/mmol compound) to which excess NaI (approx. 3.0 eq.) was added. The resulting mixture was stirred for 72h at RT. Volatiles were removed *in vacuo* to yield a yellow residue, which was extracted in DCM (240 mL/mmol compound). Evaporation of the extract yielded [(1H-benzimidazolylidene)IrCp*I₂] as a yellow powder.

Alternative protocol 2: FeCl_3 (49 mg, 0.30 mmol, 1.5 eq.) and NaI (90 mg, 0.60 mmol, 3.0 eq.) were dissolved in acetone (30 mL) to provide a black suspension. Immediately afterwards, a solution of [(2-azidophenylisonitrile)IrCp*I₂] (147 mg, 0.20 mmol, 1.0 eq.) in DCM (6 mL) was added to the black suspension and the resulting mixture was stirred for 20h at RT. Volatiles (including iodine) were removed *in vacuo* to provide a very dark red residue, which was extracted in DCM (80 mL) under atmospheric conditions. The extract was subsequently washed with a solution of $\text{Na}_2\text{S}_2\text{O}_3$ (100 mL, 20% in H_2O), a solution of NaHCO_3 (100 mL, saturated solution in H_2O) and brine (100 mL). The resulting orange solution was dried over Na_2SO_4 . After evaporation, [(1H-benzimidazolylidene)IrCp*I₂] was obtained as a dark yellow powder (96 mg, 0.14 mmol, 69%).

(κ^2 -C,N-(acetimidoyl)-benzimidazolylidene) (1,2,3,4,5-pentamethylcyclopentadienyl) iridium(III) monoiodide (8)

Alternative protocol 1 / Control reaction 1: A red solution of FeCl_3 (28 mg, 0.17 mmol, 1.9 eq.) in MeCN (6 mL) was added to a colourless solution of NaI (137 mg, 0.91 mmol, 10.1 eq.) in MeCN (6 mL). The resulting black mixture was added to an orange solution of [(1H-benzimidazolylidene)IrCp*I₂] (63 mg, 0.09 mmol, 1.0 eq.) in DCM (3 mL). The resulting black mixture was stirred for 48h at RT. Volatiles (including iodine) were removed *in vacuo* to provide a black residue, which was extracted with DCM (35 mL) under atmospheric conditions. The extract was subsequently washed with a solution of $\text{Na}_2\text{S}_2\text{O}_3$ (50 mL, 20% in H_2O) and NaHCO_3 (50 mL, saturated solution in H_2O). The resulting yellow organic layer was dried over Na_2SO_4 . After evaporation and washing with CHCl_3 (2.5 mL), [(κ^2 -C,N-(acetimidoyl)-benzimidazolylidene)IrCp*I] was obtained as a yellow powder (41 mg, 0.07 mmol, 74%).

Alternative protocol 2 / Control reaction 2: [(1H-benzimidazolylidene)IrCp*I₂] (6.5 mg, 0.0093 mmol, 1.2 eq.) was suspended in MeCN (2 mL) and refluxed for 5d. The resulting yellow solution was allowed to cool to RT and evaporated to provide [(κ^2 -C,N-1-(acetimino)-benzimidazolylidene) IrCp*I₂] as an oily orange-yellow solid, which then was dissolved in THF (3.9 mL) and cooled to -78°C . A solution of DBU (0.1 mL of a 0.08M solution in THF, 1.0 eq.) in THF (0.1 mL) was added dropwise. The resulting yellow solution was allowed to warm to RT and was stirred for 60 min. Evaporation provided a yellow solid, which was washed with CHCl_3 (0.5 mL) to provide [(κ^2 -C,N-(acetimidoyl)-benzimidazolylidene)IrCp*I] as a light yellow powder (1.5 mg, 0.0026 mmol, 32%).

Control reaction 3: [(2-azidophenylisonitrile)IrCp*I₂] (90 mg, 0.12 mmol, 1.0 eq.) and NaI (190 mg, 1.27 mmol, 10.6 eq.) were dissolved in MeCN (13 mL) to provide a brown suspension. A red solution of FeCl_3 (36 mg, 0.22 mmol, 1.8 eq.) in MeCN (12 mL) was added to provide a very dark brown mixture which was stirred for 49h at RT. Volatiles (including iodine) were removed *in vacuo* to provide a black solid, which was extracted in DCM (2 x 30 mL) under atmospheric conditions. The extract was subsequently washed with a solution of $\text{Na}_2\text{S}_2\text{O}_3$ (60 mL, 20% in H_2O) and NaHCO_3 (60 mL, saturated solution in H_2O). The resulting orange solution was dried over Na_2SO_4 and evaporated to provide an orange solid, which was washed with CHCl_3 (10 mL), Et_2O (20mL) and pentane (20 mL). $^1\text{H-NMR}$ analysis of the obtained orange solid (49 mg) revealed a mixture of [(κ^2 -C,N-(acetimidoyl)-benzimidazolylidene)IrCp*I] and [(1H-benzimidazolylidene)IrCp*I₂].

Bis ((1,2,3,4,5-pentamethylcyclopentadienyl) iridium(III)) (μ -hydrido) di(μ - κ^2 -C,N-1H-benzimidazolylidene) mono-chloride (9)

Alternative protocol 1 / Control reaction 1: [(1H-benzimidazolylidene)IrCp*Cl₂] (6.5 mg, 0.01 mmol, 1.0 eq.) was suspended in MeOH (1 mL) to provide an orange mixture, to which zinc dust (2 mg, 0.03 mmol, 3 eq.) and H_2O (0.01 mL) were added. The mixture was stirred at reflux for 7d to provide an orange/red solution, which was allowed to cool to RT and was evaporated to provide a red solid. Under atmospheric conditions, the solid was extracted into CD_2Cl_2 (3.0 mL), after which evaporation provided μ - κ^2 -C,N-1H-benzimidazolylidene)₂Ir₂Cp*₂(μ -H)Cl] as a red solid (quant.).

Control reaction 2: [(2-azidophenylisonitrile)IrCp*I₂] (65 mg, 0.09 mmol, 1.0 eq.) was suspended in MeOH (20 mL) to provide an orange mixture, which was added over NH_4Cl (13 mg, 0.24 mmol, 2.7 eq.) and zinc dust (10 mg, 0.15 mmol, 1.7 eq.). H_2O (0.2 mL) was added and the suspension was stirred at reflux for 7d to provide a brown solution, which was allowed to cool to RT and was evaporated. Under atmospheric conditions, the brown solid was extracted in DCM (10 mL + 5 mL) and the combined extracts were evaporated to

provide an orange powder, which was washed with Et₂O (15 mL) and pentane (15 mL). The powder was dissolved in DCM (20 mL) and washed with H₂O (20 mL). Evaporation of the organic layer provided a red powder. ¹H-NMR analysis showed no [(μ-κ²-C,N-1H-benzimidazolyli-dene)₂Ir₂Cp*₂(μ-H)X] formation.

Control reaction 3: [(1H-benzimidazolyli-dene)IrCp*Cl₂] (6.5 mg, 0.01 mmol, 1.0 eq.) was suspended in MeOH (1 mL) to provide an orange mixture, to which H₂O (0.01 mL) was added. The mixture was stirred at reflux for 7d to provide an orange solution, which was allowed to cool to RT and evaporated to yield a red solid. ¹H-NMR analysis showed no [(μ-κ²-C,N-1H-benzimidazolyli-dene)₂Ir₂Cp*₂(μ-H)Cl] formation.

Attempted synthesis (3-benzimidazolyl) (1,2,3,4,5-pentamethylcyclopentadienyl) iridium(III) dichloride

To a white suspension of benzimidazole (20 mg, 0.17 mmol, 3.4 eq.) in DCM (5 mL) was added [IrCp*Cl₂]₂ (38 mg, 0.05 mmol, 1.0 eq.) to provide a yellow suspension, which was stirred for 2 days at RT. Evaporation yielded a yellow solid, which was washed with Et₂O (3 x 2 mL) to provide a white-yellow solid (22 mg, 0.04 mmol, 44%). The extremely low solubility of the product prevented further identification.

Attempted synthesis bis((1,2,3,4,5-pentamethylcyclopentadienyl) rhodium(III)) (μ-hydrido) di(μ-κ²-C,N-1H-benzimidazolyli-dene) monochloride

[(2-azidophenylisonitrile)RhCp*Cl₂] (56 mg, 0.12 mmol, 1.0 eq.), NH₄Cl (26.2 mg, 0.49 mmol, 4.1 eq.) and zinc dust (20 mg, 0.30 mmol, 2.5 eq.) were combined in MeOH (15 mL) to give a red suspension, to which H₂O (0.12 mL) was added. The resulting mixture was stirred at reflux for 164 hr to provide a red solution, which was allowed to cool to RT and was evaporated. The resulting red powder was washed with pentane (1 x 10 mL, 2 x 6 mL) and Et₂O (2 x 10 mL). Under atmospheric conditions, the residue was dissolved in DCM (60 mL) and washed with H₂O (3 x 60 mL, 1 x 40 mL). The organic layer was dried and evaporated to provide a red solid. ¹H-NMR analysis showed no bis((1,2,3,4,5-pentamethylcyclopentadienyl) rhodium(III)) (μ-hydrido) di(μ-κ²-C,N-1H-benzimidazolyli-dene) monochloride formation but a mixture of [(1H-benzimidazolyli-dene)RhCp*Cl₂] and unidentified side-products.

Attempted synthesis bis((1-methyl-4-isopropyl-benzene) ruthenium(II)) (μ-hydrido) di(μ-κ²-C,N-1H-benzimidazolyli-dene) monochloride

Protocol 1: [Ru(*p*-cymene)(2-azidophenylisonitrile)Cl₂] (74 mg, 0.16 mmol, 1.0 eq.), NH₄Cl (35 mg, 0.64 mmol, 4.0 eq.) and zinc dust (26 mg, 0.40 mmol, 2.5 eq.) were combined in MeOH (16 mL) to provide a yellow/brown suspension to which H₂O (0.17 mL) was added. The mixture was stirred at reflux for 165 hr to provide a black suspension, which was allowed to cool to RT and was evaporated. Washing with Et₂O (3 x 10 mL) provided a black powder (0% bis((1-methyl-4-isopropyl-benzene) ruthenium(II)) (μ-hydrido) di(μ-κ²-C,N-1H-benzimidazolyli-dene) monochloride). ¹H-NMR analysis revealed decomposition.

Protocol 2: [Ru(*p*-cymene)(2-azidophenylisonitrile)Cl₂] (78 mg, 0.17 mmol, 1.0 eq.), NH₄Cl (36 mg, 0.66 mmol, 3.9 eq.) and zinc dust (26 mg, 0.40 mmol, 2.4 eq.) were combined in MeOH (17 mL) to provide a yellow/brown suspension to which H₂O (0.17 mL) was added. The mixture was stirred at RT for 164 hr to provide a black suspension, which was allowed to cool to RT and was evaporated. Washing with Et₂O (3 x 10 mL) provided a black powder (0% bis((1-methyl-4-isopropyl-benzene) ruthenium(II)) (μ-hydrido) di(μ-κ²-C,N-1H-benzimidazolyli-dene) monochloride; partial formation of (1H-benzimidazolyli-dene) Ru(II)(*p*-cymene)Cl₂;⁷ HRMS (ESI-Q-TOF): calcd. for C₁₇H₂₂ClN₂Ru: 391.0515; found: 391.0345).

⁷ For the corresponding diiodo complex see: O. Kaufhold, A. Flores-Figueroa, T. Pape, F.E. Hahn, *Organometallics*, **2009**, *28*, 896.

2. NMR-spectra

General considerations

NMR spectra were recorded on Bruker Avance 400 (^1H , 400.13 MHz; $^{13}\text{C}\{^1\text{H}\}$, 100.61 MHz, room temperature) or a Bruker Avance 500 (^1H , 500.23 MHz; $^{13}\text{C}\{^1\text{H}\}$, 125.78 MHz; room temperature). Chemical shifts are reported in ppm downfield from tetramethylsilane. ^1H -spectra were internally referenced to residual solvent resonances: CDCl_3 (δ 7.26) and CD_2Cl_2 (δ 5.32). ^{13}C -spectra were internally referenced to residual solvent resonances: CDCl_3 (δ 77.16) and CD_2Cl_2 (δ 53.84).

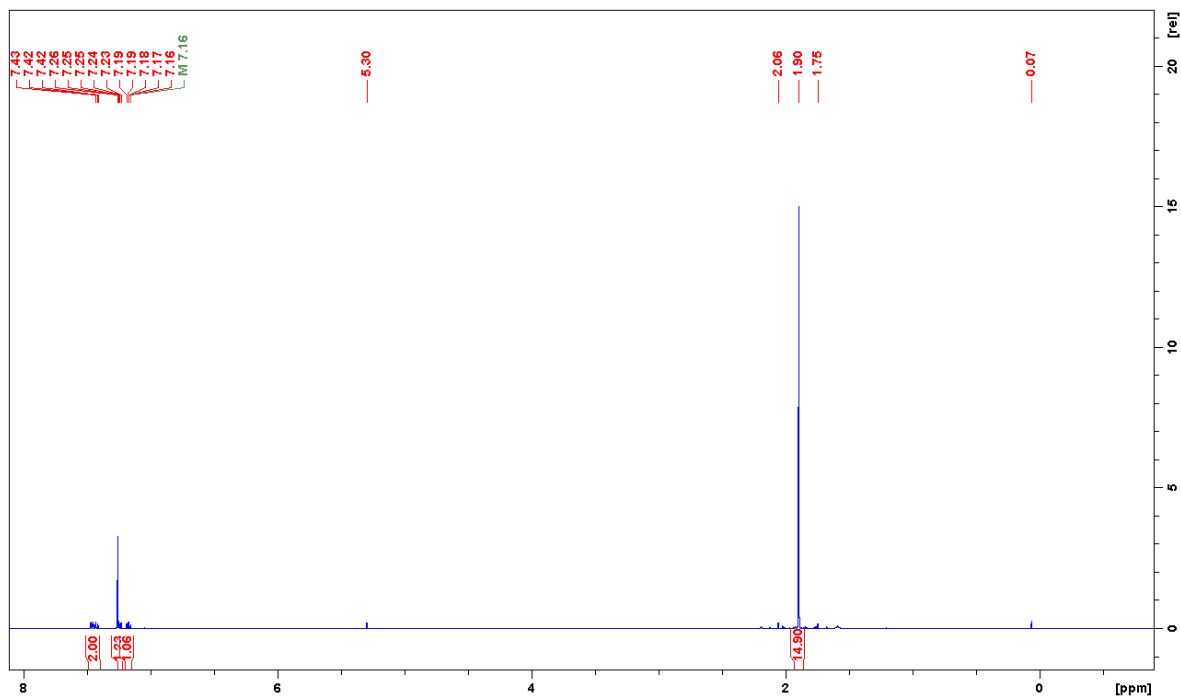


Figure S1. ^1H -NMR (500.23 MHz, CDCl_3) of complex 2.

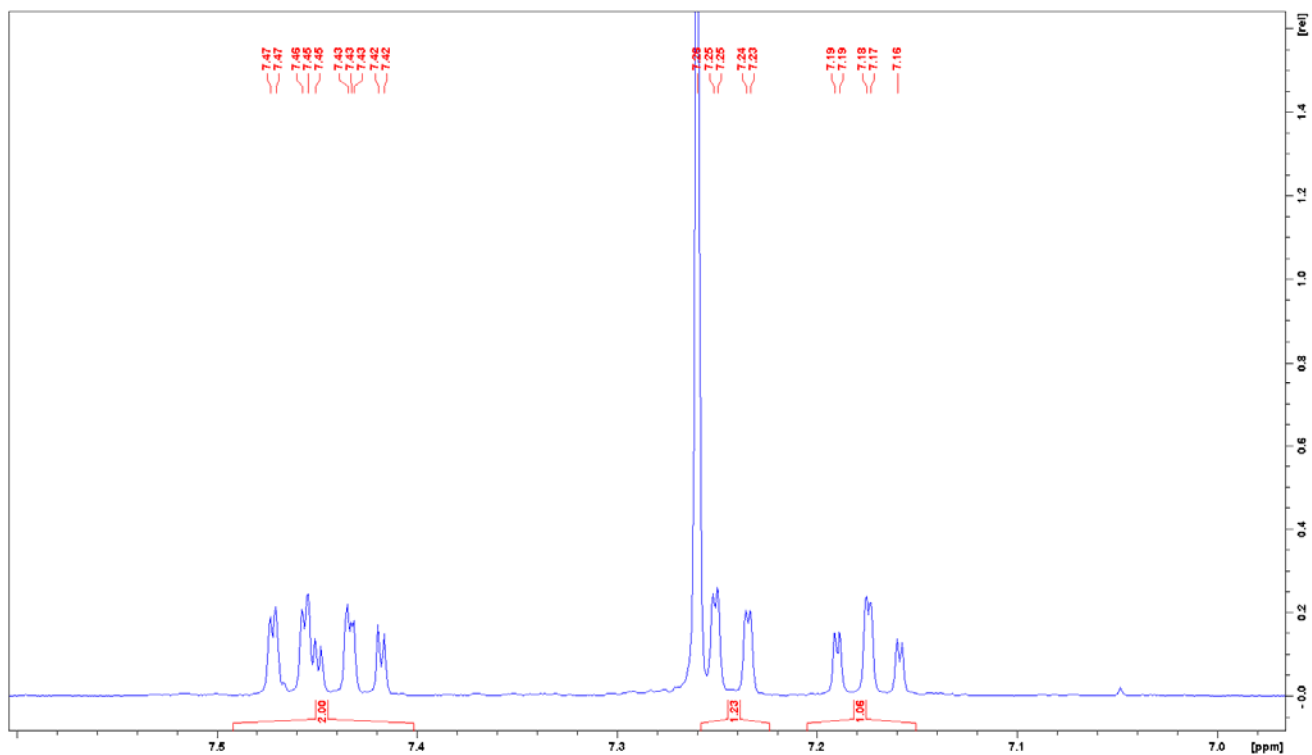


Figure S2. Aromatic region ^1H -NMR (500.23 MHz, CDCl_3) of complex **2**.

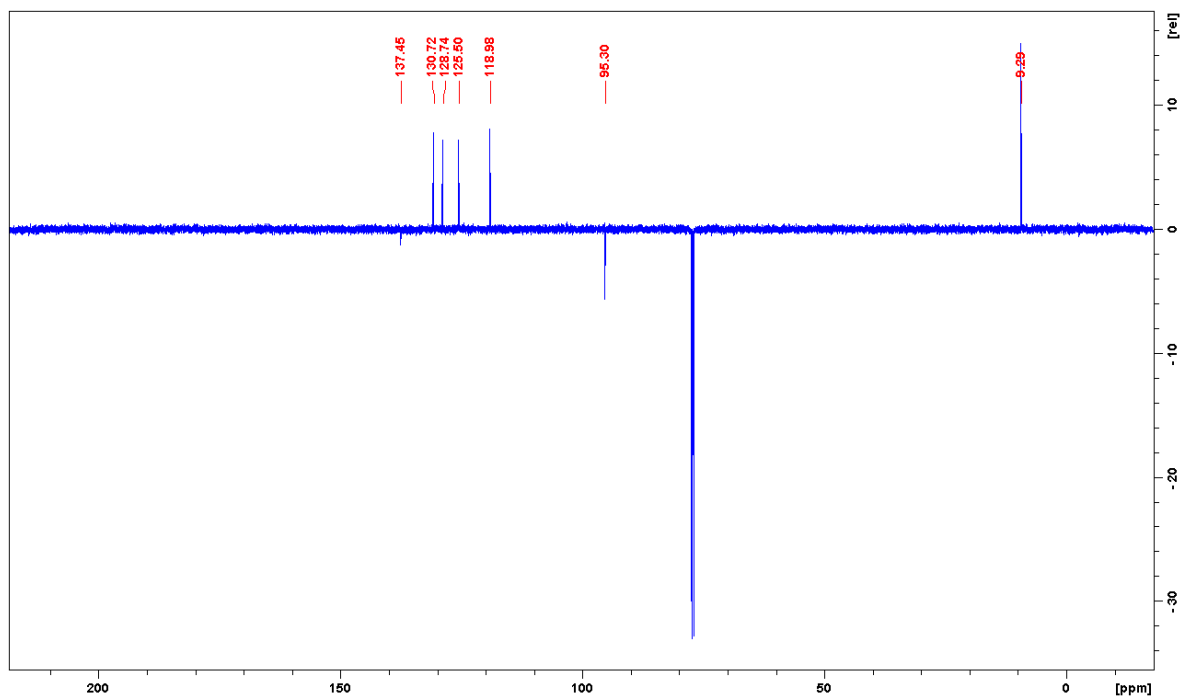


Figure S3. $^{13}\text{C}\{^1\text{H}\}$ -NMR (125.78 MHz, CDCl_3) of complex **2**.

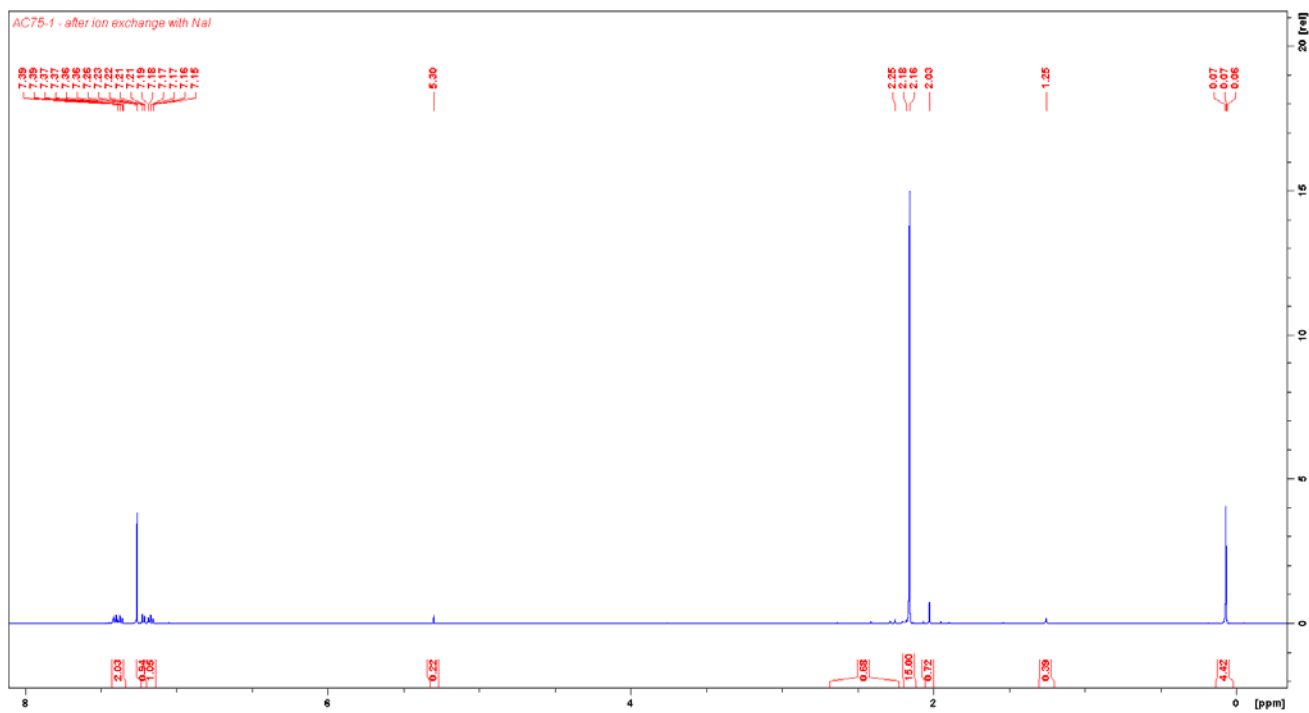


Figure S4. $^1\text{H-NMR}$ (500.23 MHz, CDCl_3) of complex **3**.

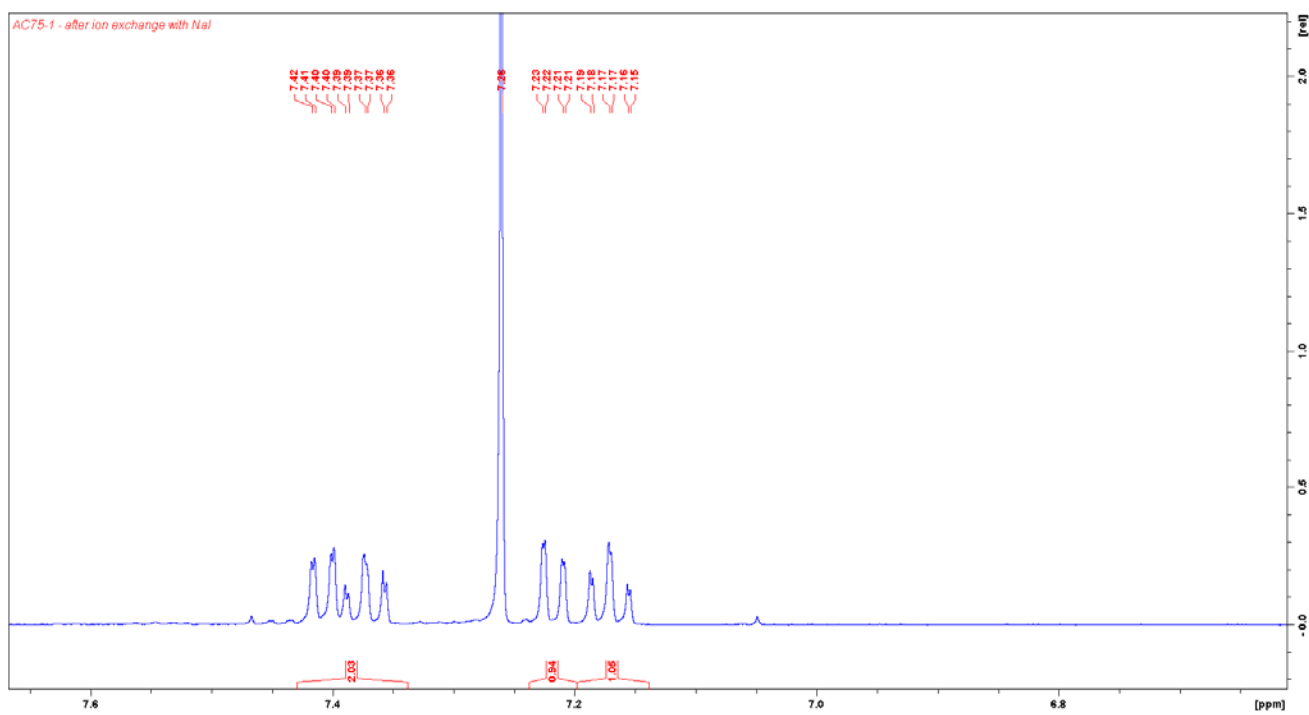


Figure S5. Aromatic region $^1\text{H-NMR}$ (500.23 MHz, CDCl_3) of complex **3**.

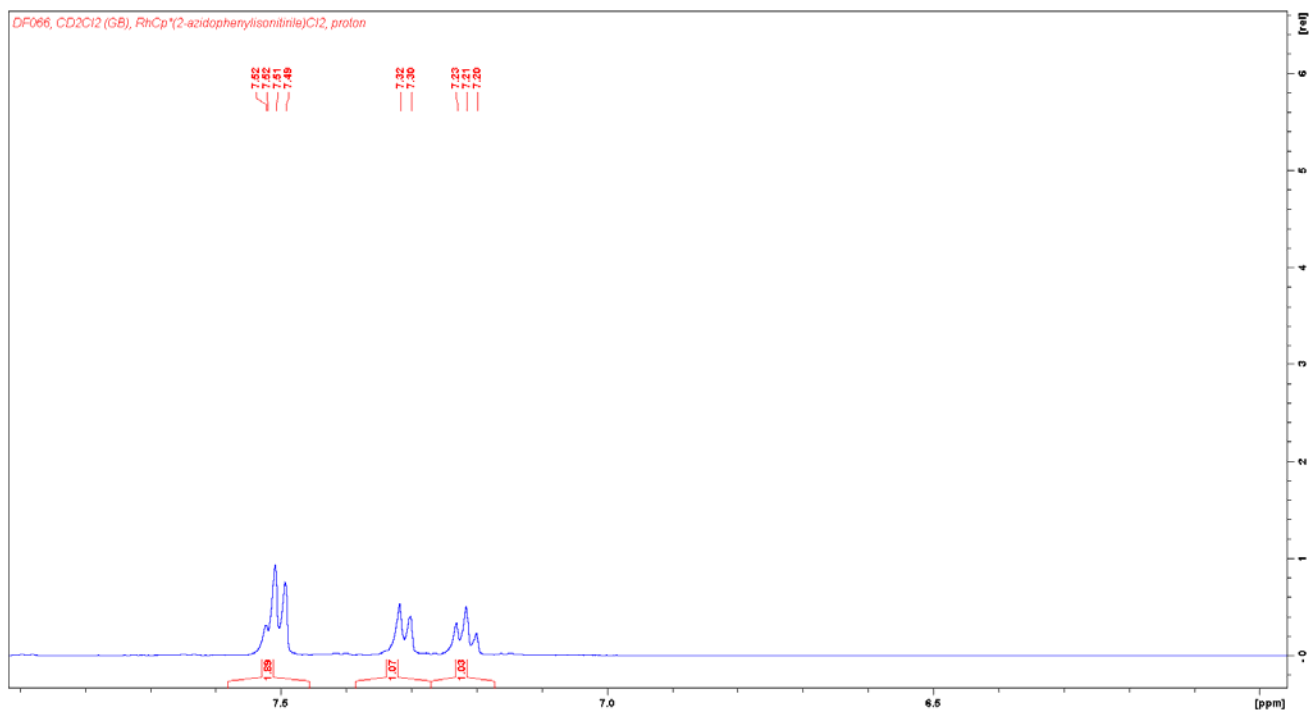


Figure S8. Aromatic region ^1H -NMR (500.23 MHz, CDCl_3) of (2-azidophenylisonitrile) (1,2,3,4,5-pentamethylcyclopentadienyl) rhodium(III) dichloride.

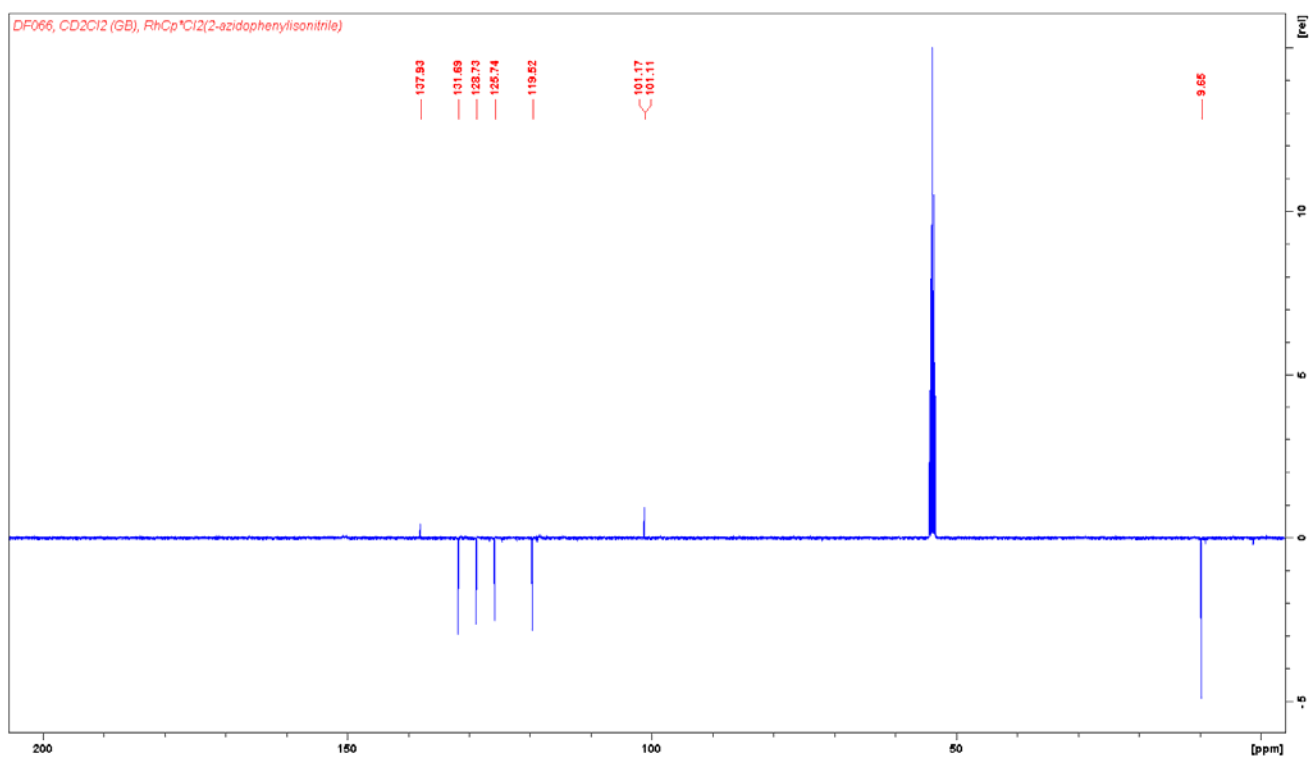


Figure S9. $^{13}\text{C}\{^1\text{H}\}$ -NMR (125.78 MHz, CDCl_3) of (2-azidophenylisonitrile) (1,2,3,4,5-pentamethylcyclopentadienyl) rhodium(III) dichloride.

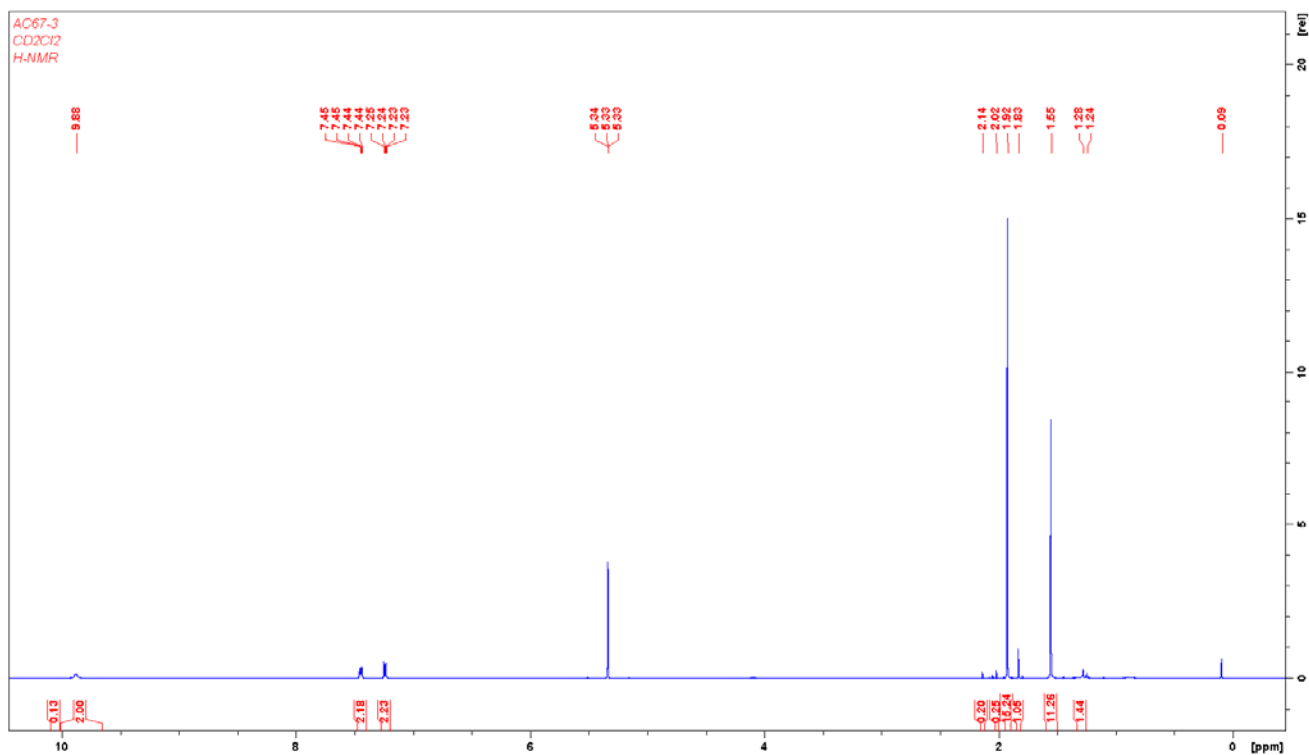


Figure S10. ¹H-NMR (500.23 MHz, CD₂Cl₂) of complex 4.

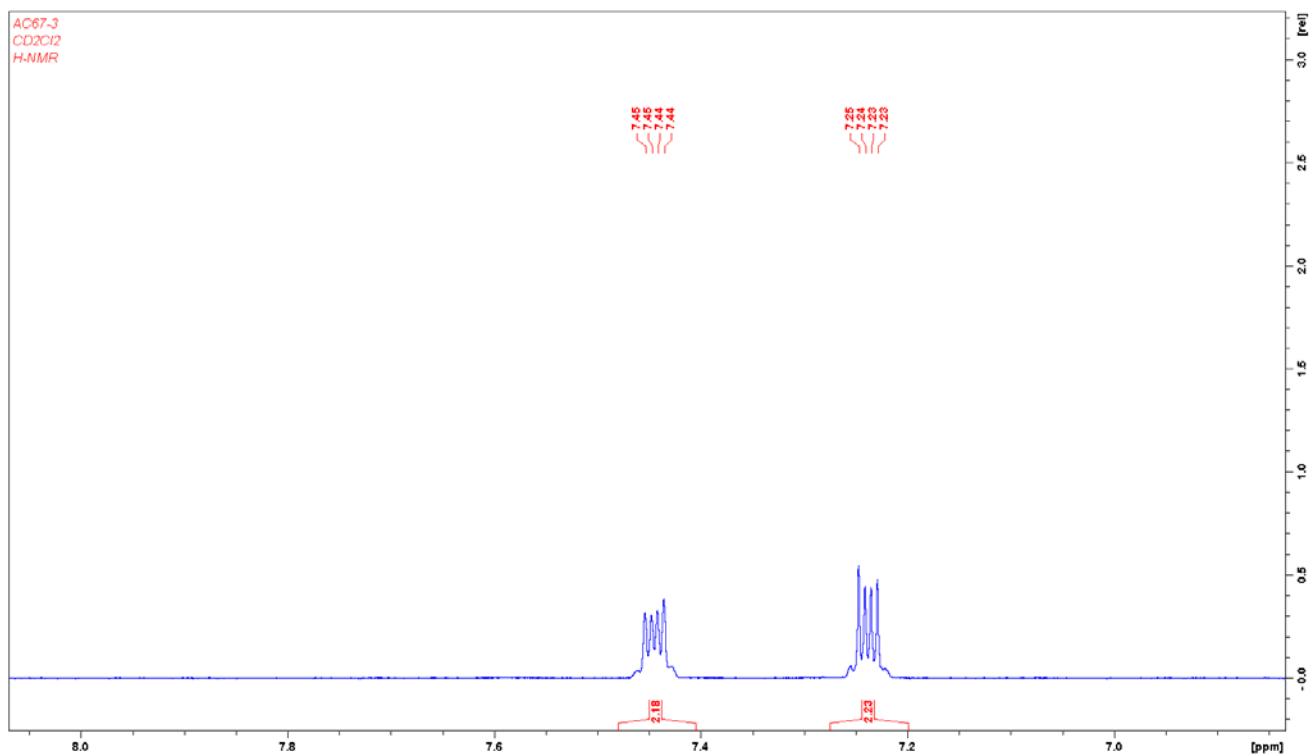


Figure S11. Aromatic region ¹H-NMR (500.23 MHz, CD₂Cl₂) of complex 4.

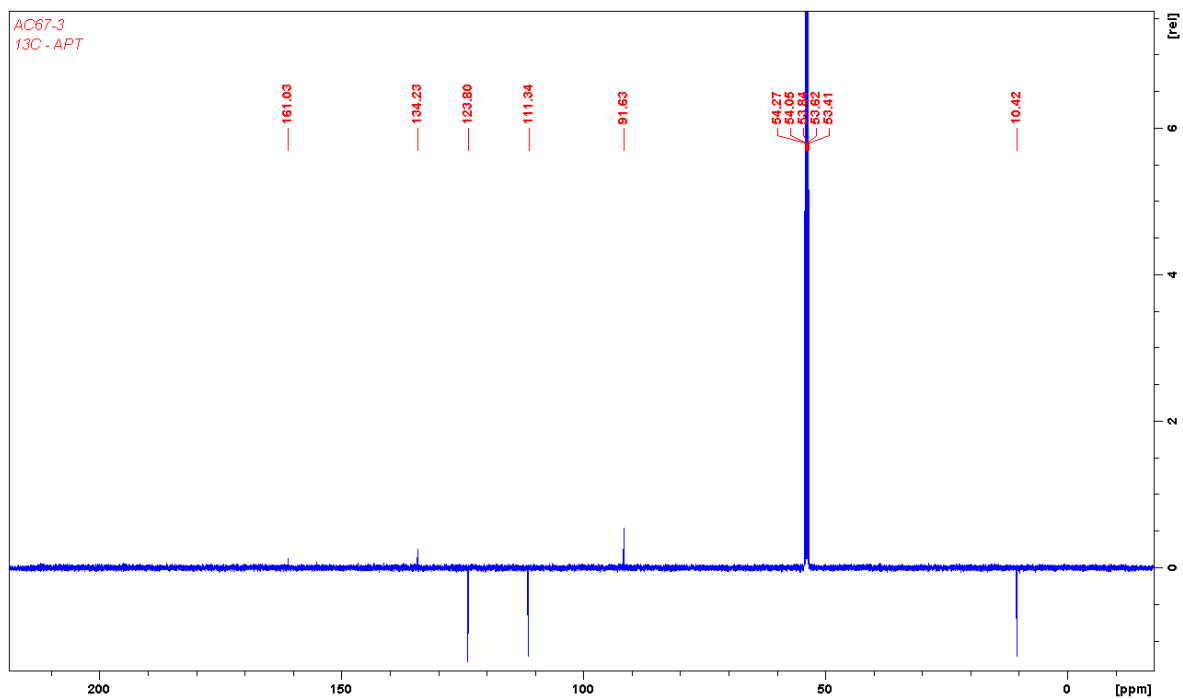


Figure S12. $^{13}\text{C}\{^1\text{H}\}$ -NMR (125.78 MHz, CD_2Cl_2) of complex 4.

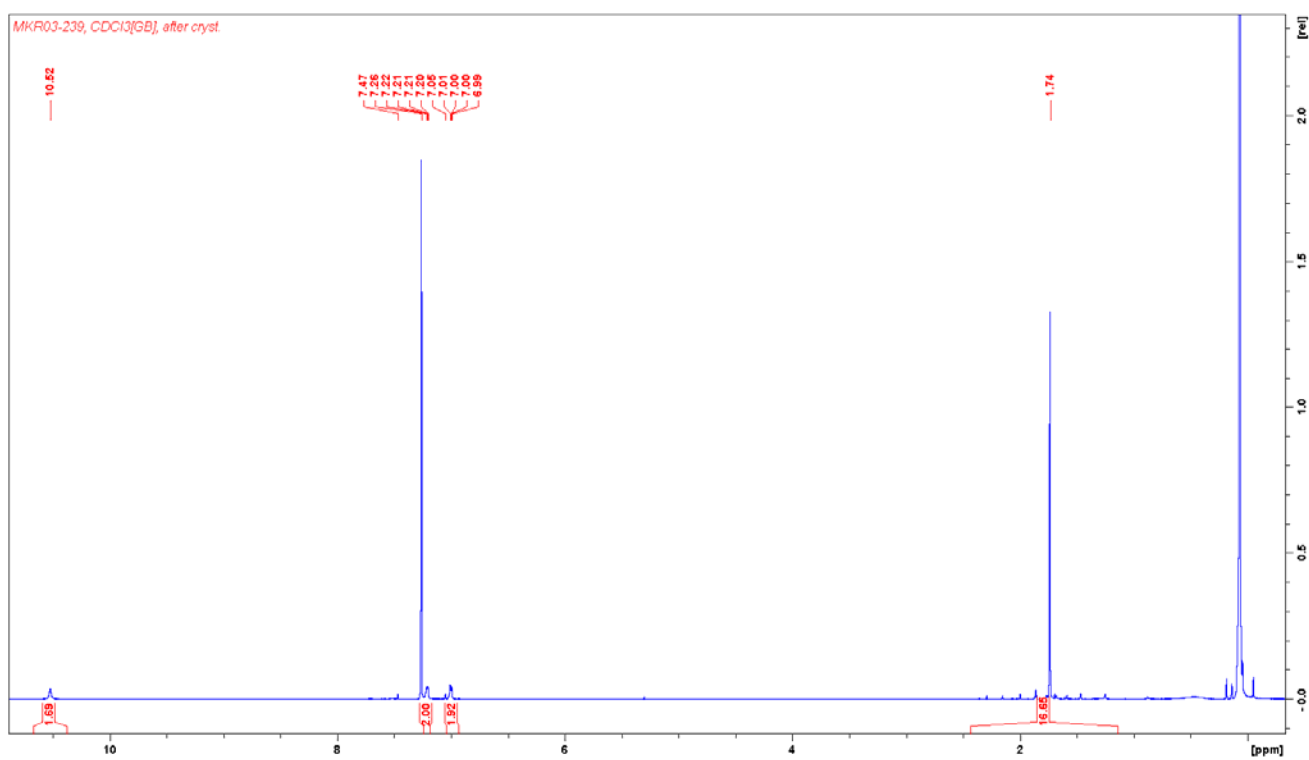


Figure S13. ^1H -NMR (500.23 MHz, CDCl_3) of complex 5.

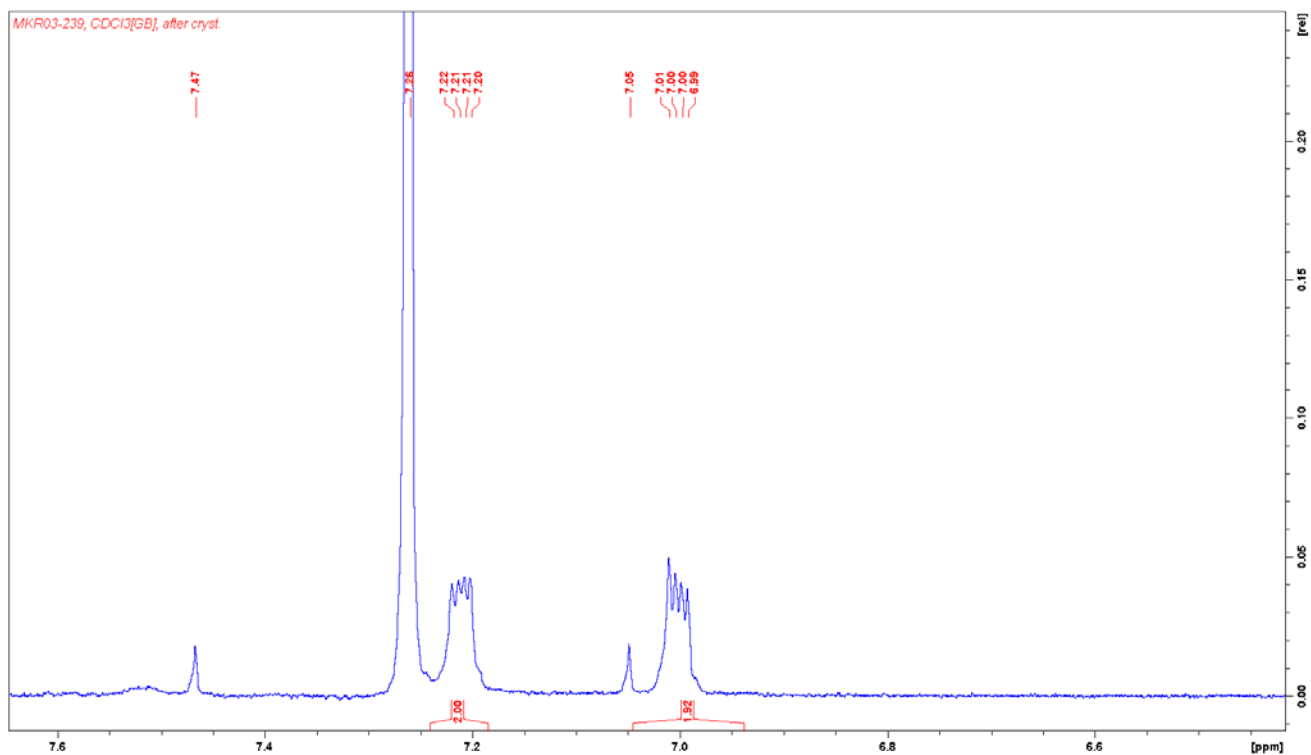


Figure S14. Aromatic region $^1\text{H-NMR}$ (500.23 MHz, CDCl_3) of complex 5.

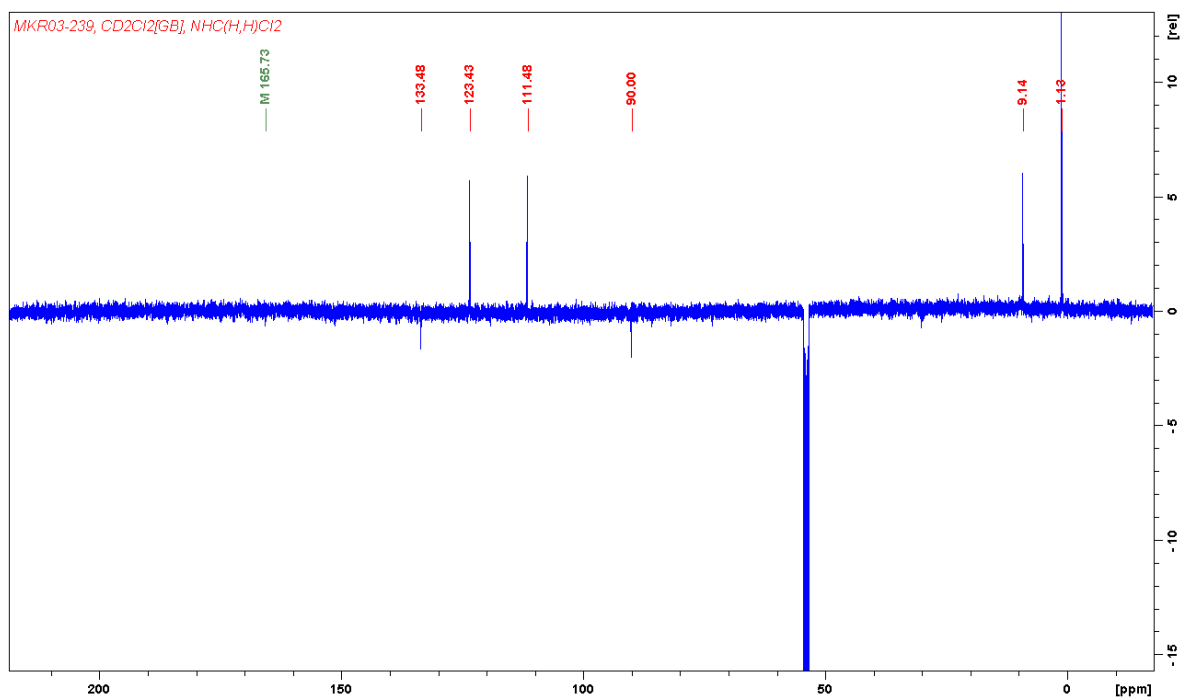


Figure S15. $^{13}\text{C}\{^1\text{H}\}$ -NMR (125.78 MHz, CD_2Cl_2) of complex 5.

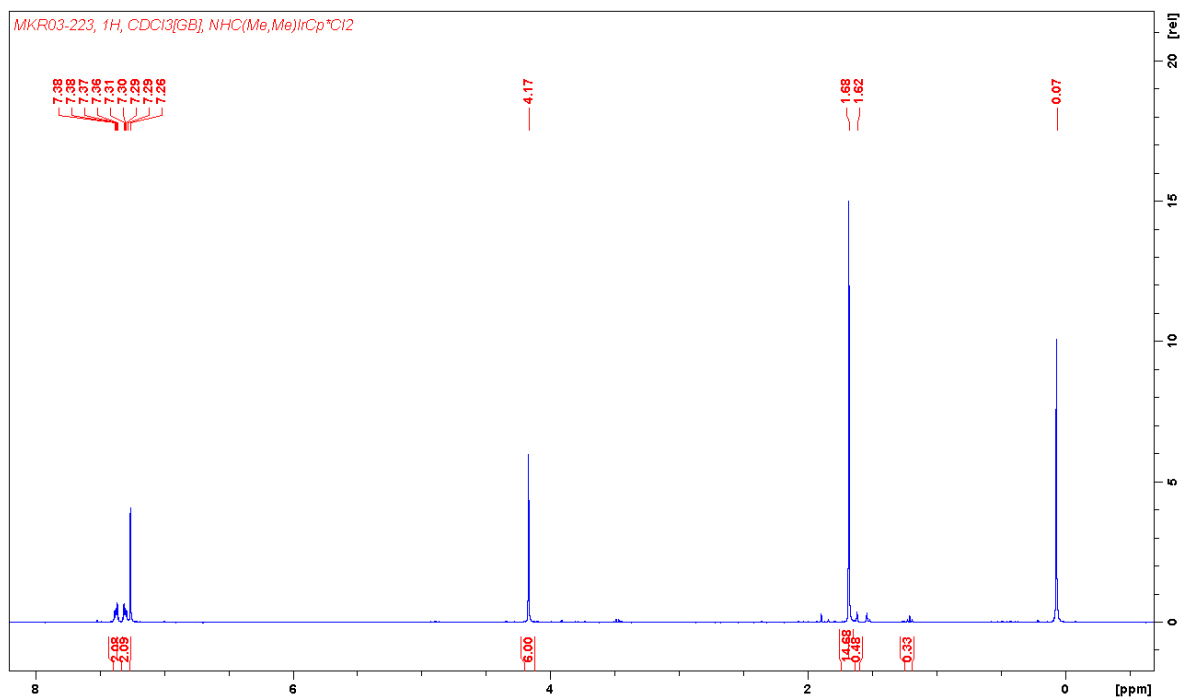


Figure S16. $^1\text{H-NMR}$ (400.13 MHz, CDCl_3) of $(N,N'$ -dimethyl-2-benzimidazolylidene) (1,2,3,4,5-pentamethylcyclopentadienyl) iridium(III) dichloride.

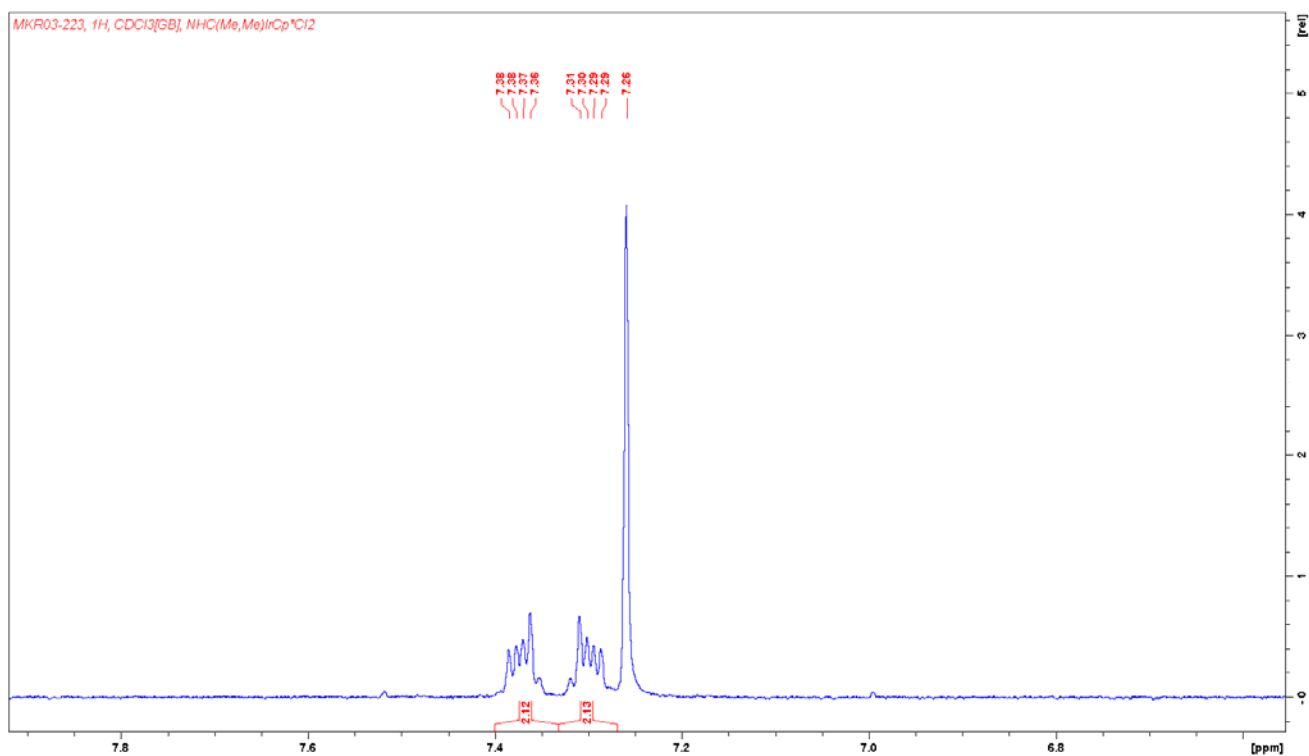


Figure S17. Aromatic region $^1\text{H-NMR}$ (400.13 MHz, CDCl_3) of $(N,N'$ -dimethyl-2-benzimidazolylidene) (1,2,3,4,5-pentamethylcyclopentadienyl) iridium(III) dichloride.

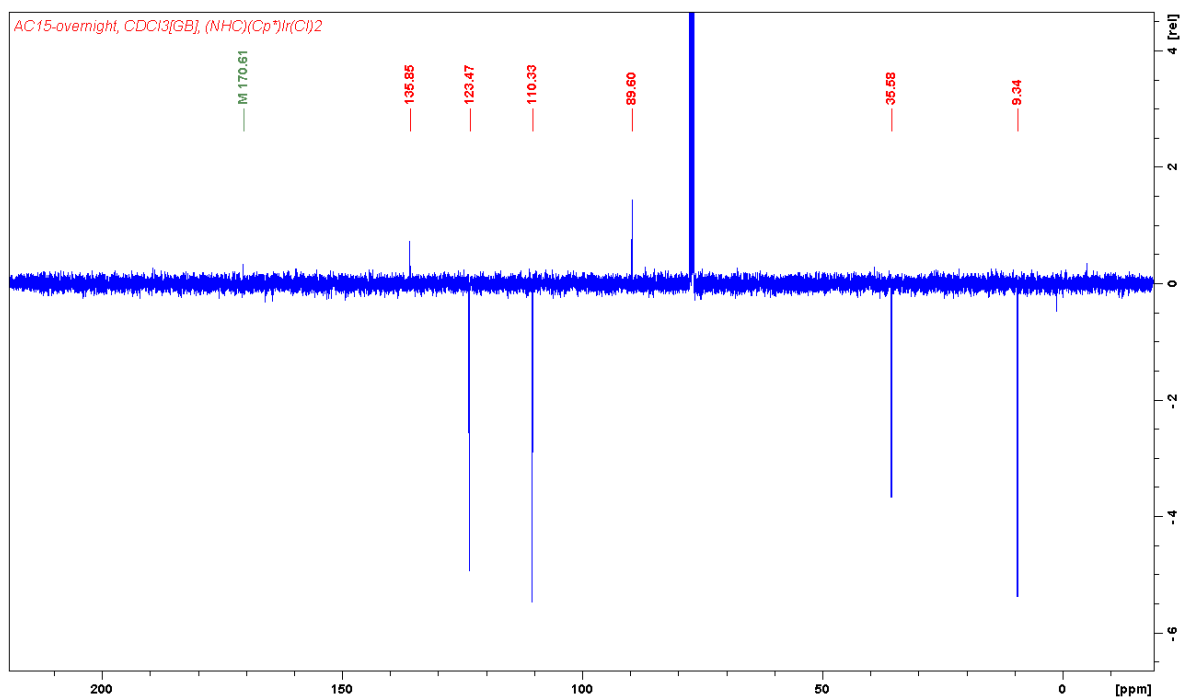


Figure S18. $^{13}\text{C}\{^1\text{H}\}$ -NMR (100.61 MHz, CDCl_3) of (*N,N'*-dimethyl-2-benzimidazolylidene) (1,2,3,4,5-pentamethylcyclopentadienyl) iridium(III) dichloride.

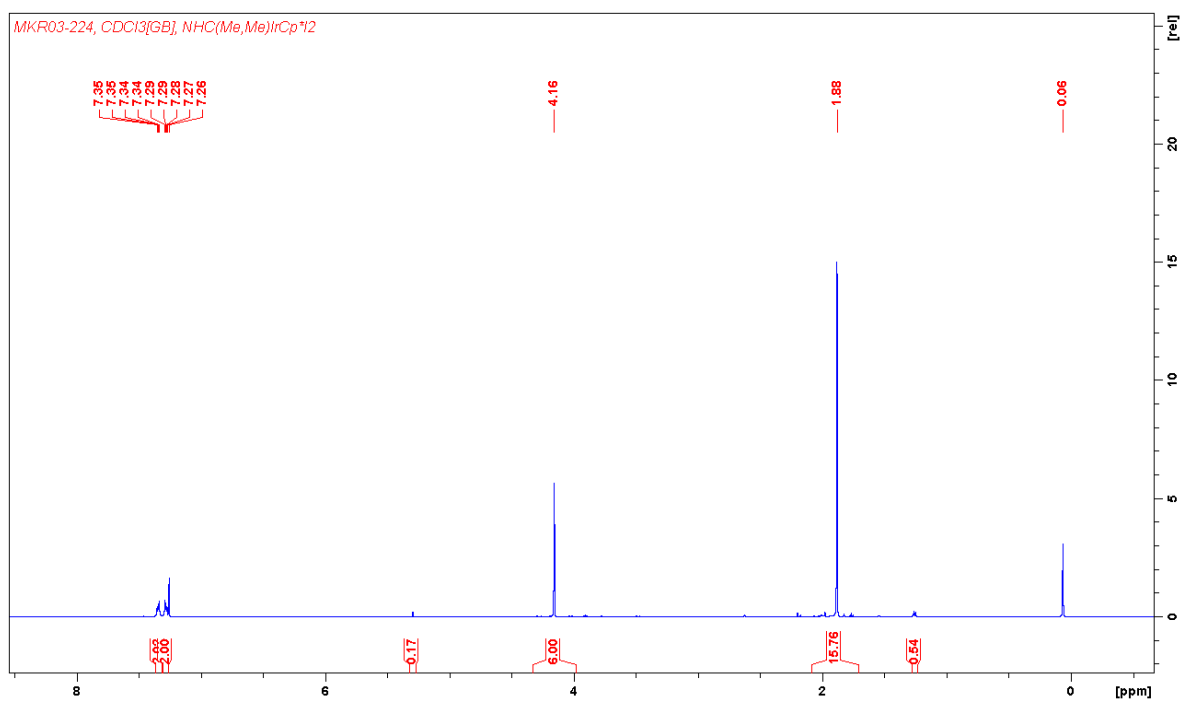


Figure S19. ^1H -NMR (500.23 MHz, CDCl_3) of complex 6.

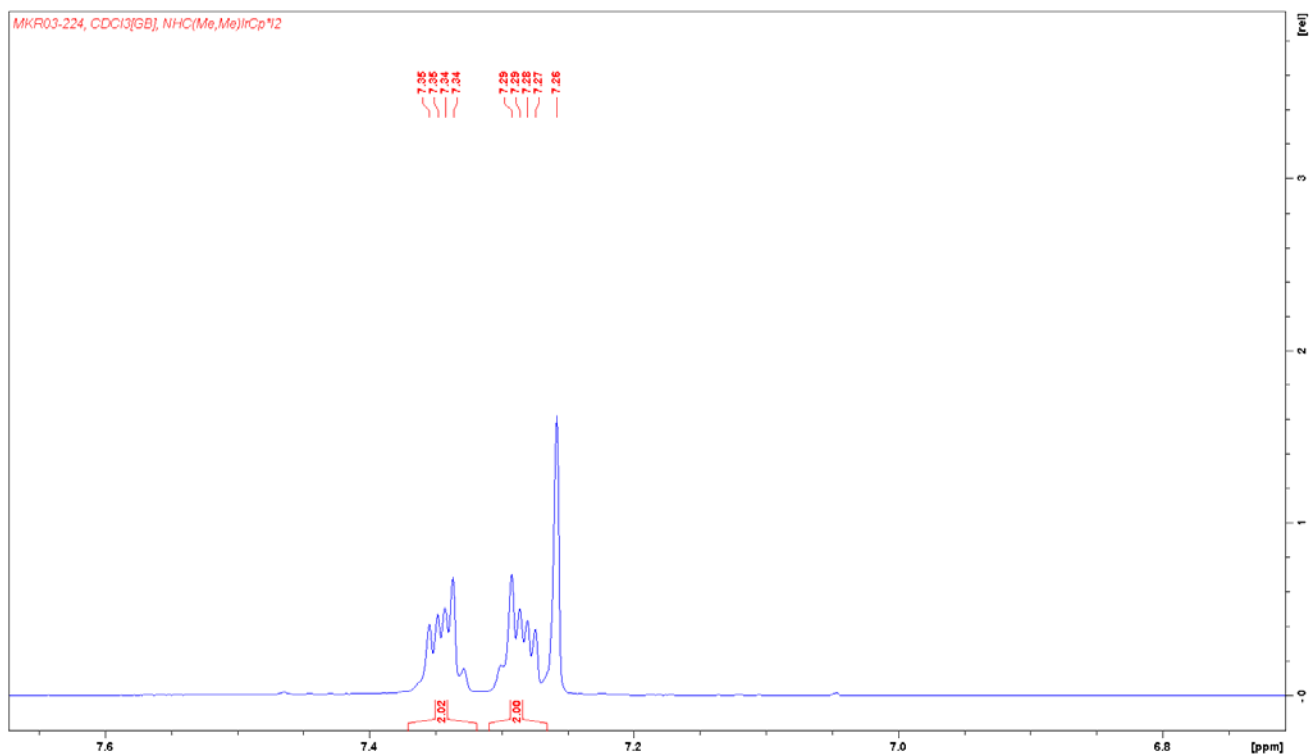


Figure S20. Aromatic region ¹H-NMR (500.23 MHz, CDCl₃) of complex **6**.

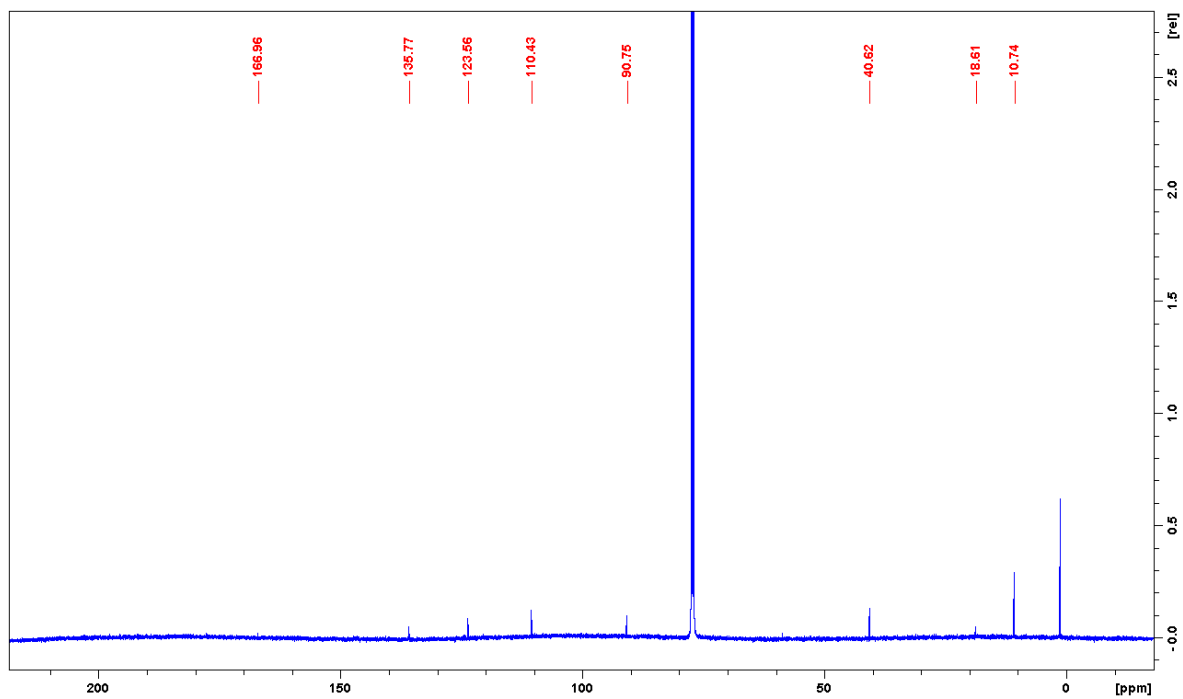


Figure S21. ¹³C{¹H}-NMR (125.78 MHz, CDCl₃) of complex **6**.

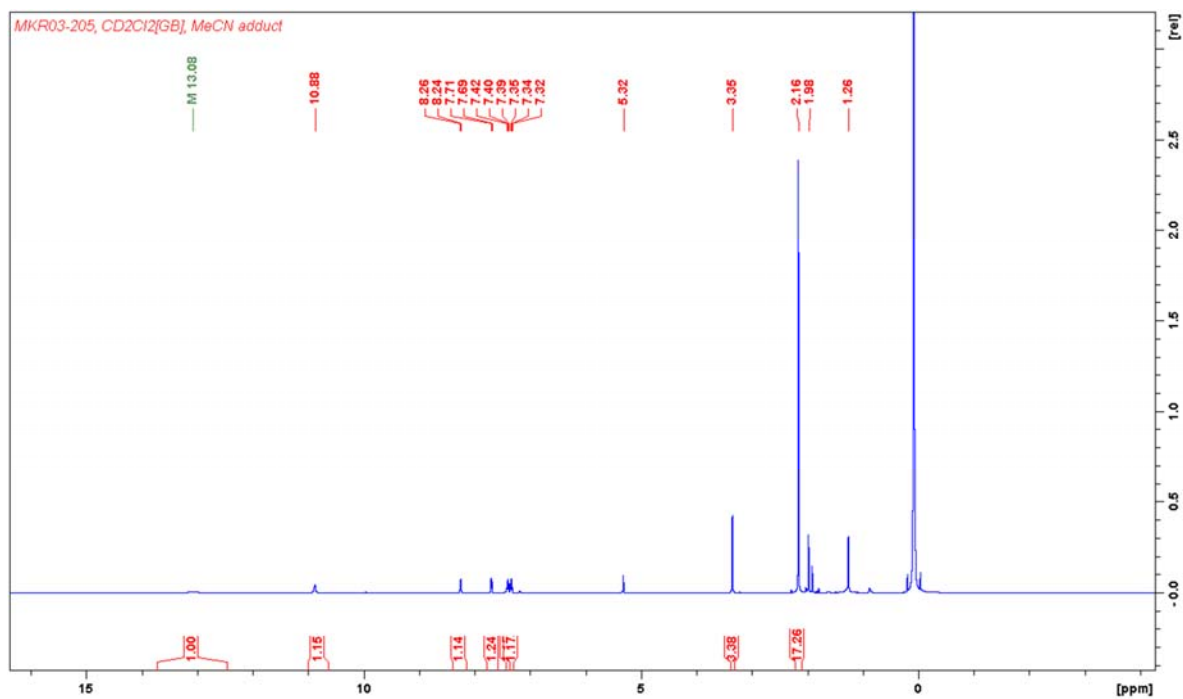


Figure S22. $^1\text{H-NMR}$ (500.23 MHz, CD_2Cl_2) of complex 7.

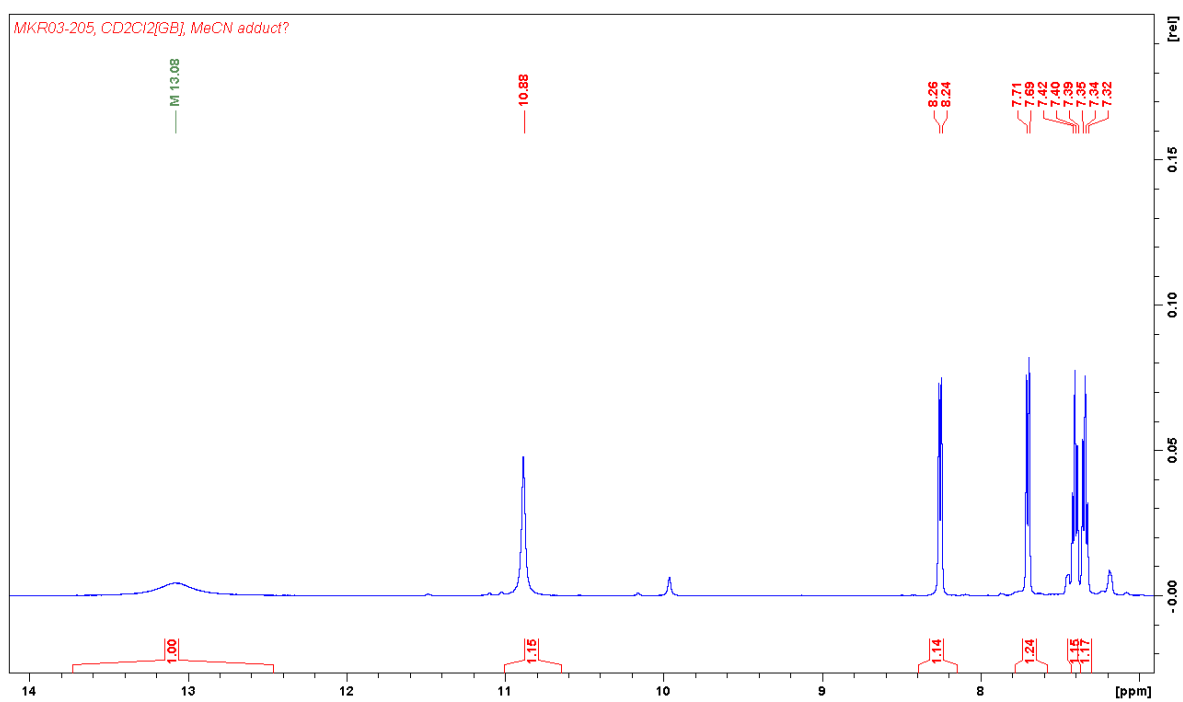


Figure S23. Aromatic region $^1\text{H-NMR}$ (500.23 MHz, CD_2Cl_2) of complex 7.

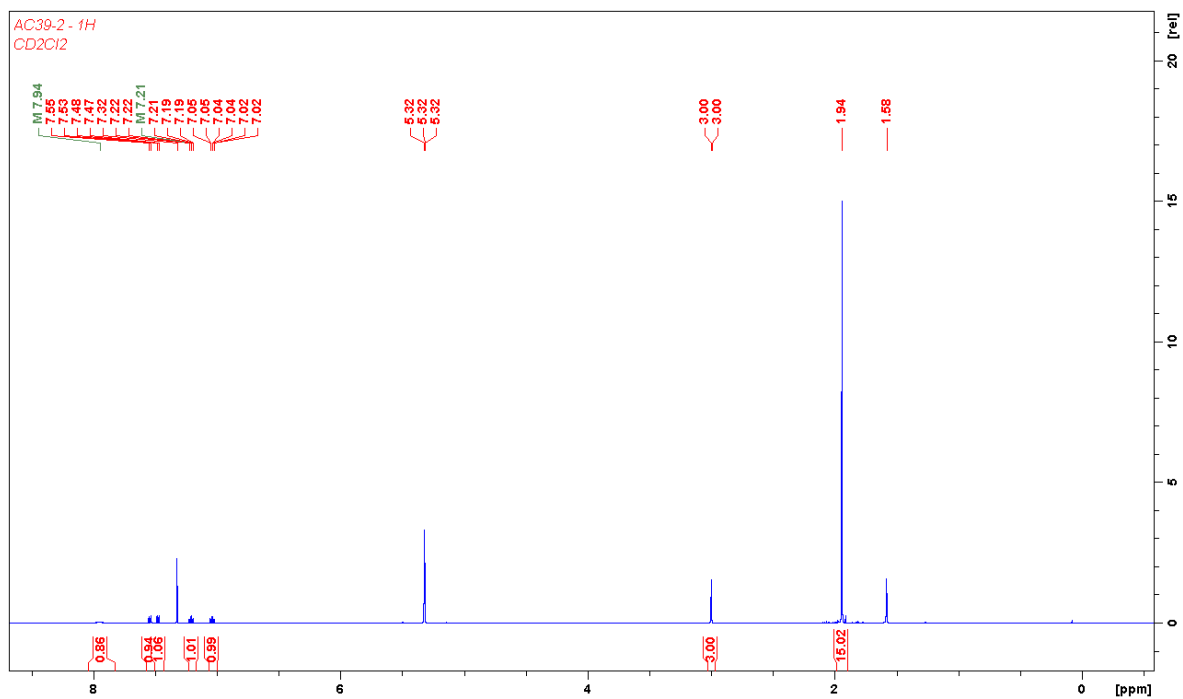


Figure S24. ¹H-NMR (500.23 MHz, CD₂Cl₂) of complex **8**.

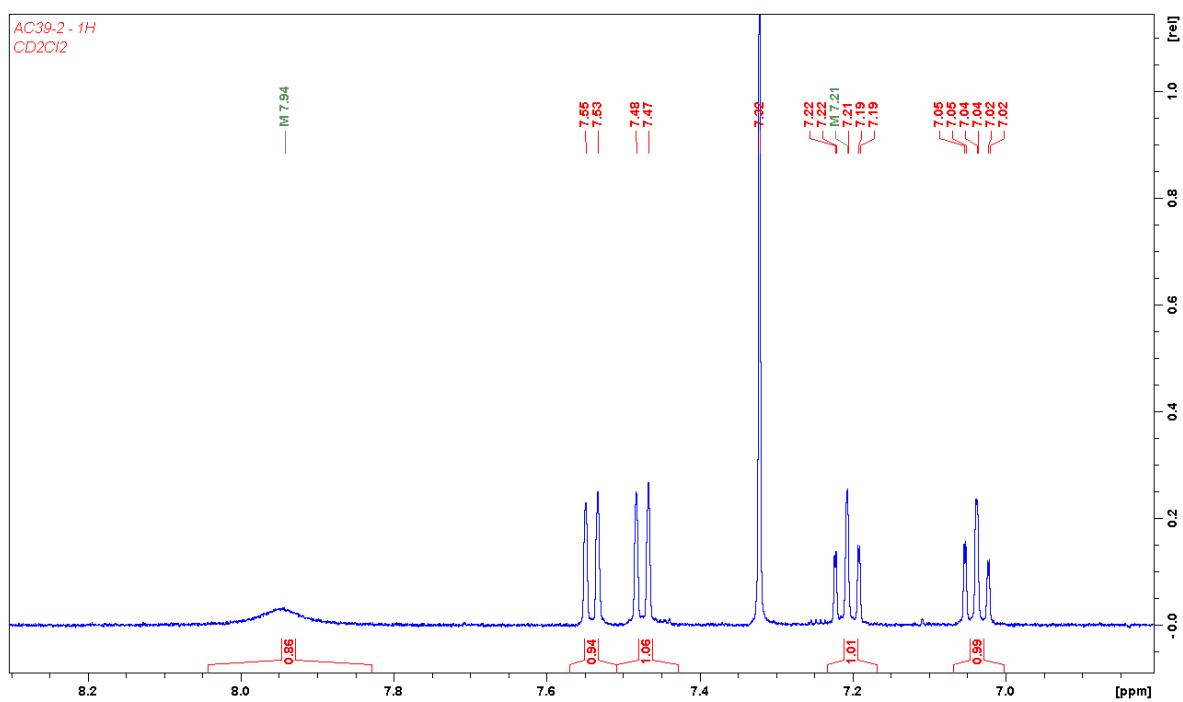


Figure S25. Aromatic region ¹H-NMR (500.23 MHz, CD₂Cl₂) of complex **8**.

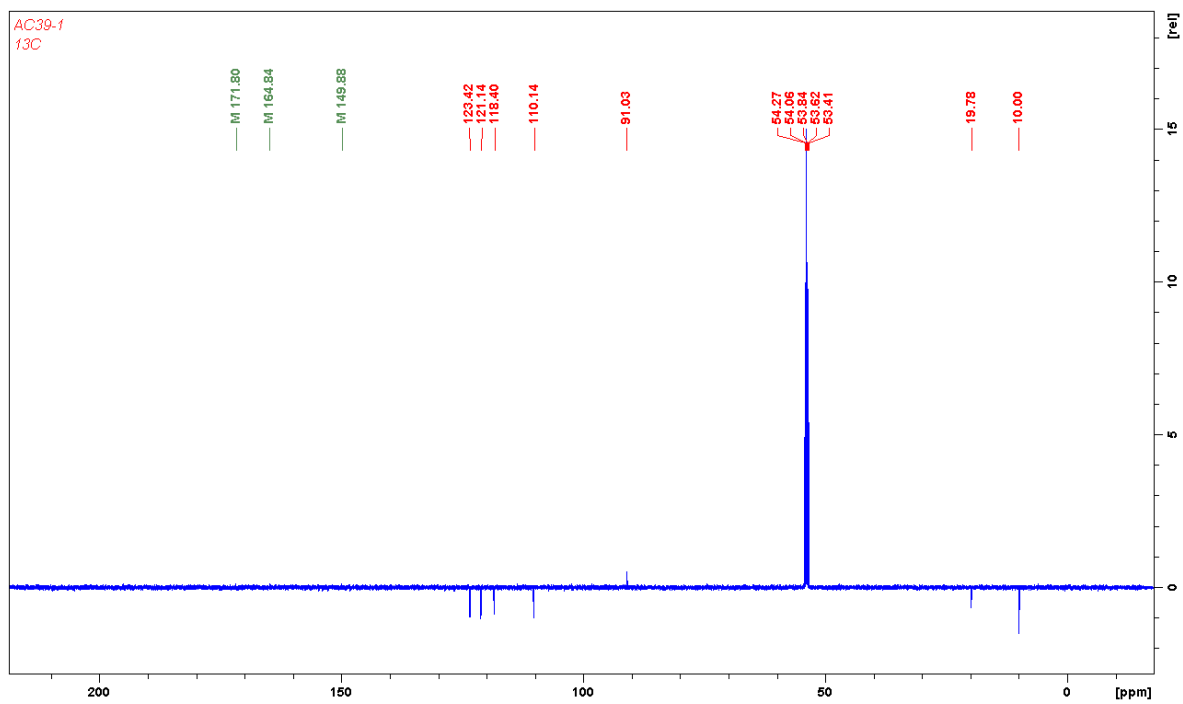


Figure S26. $^{13}\text{C}\{^1\text{H}\}$ -NMR (125.78 MHz, CD_2Cl_2) of complex **8**.

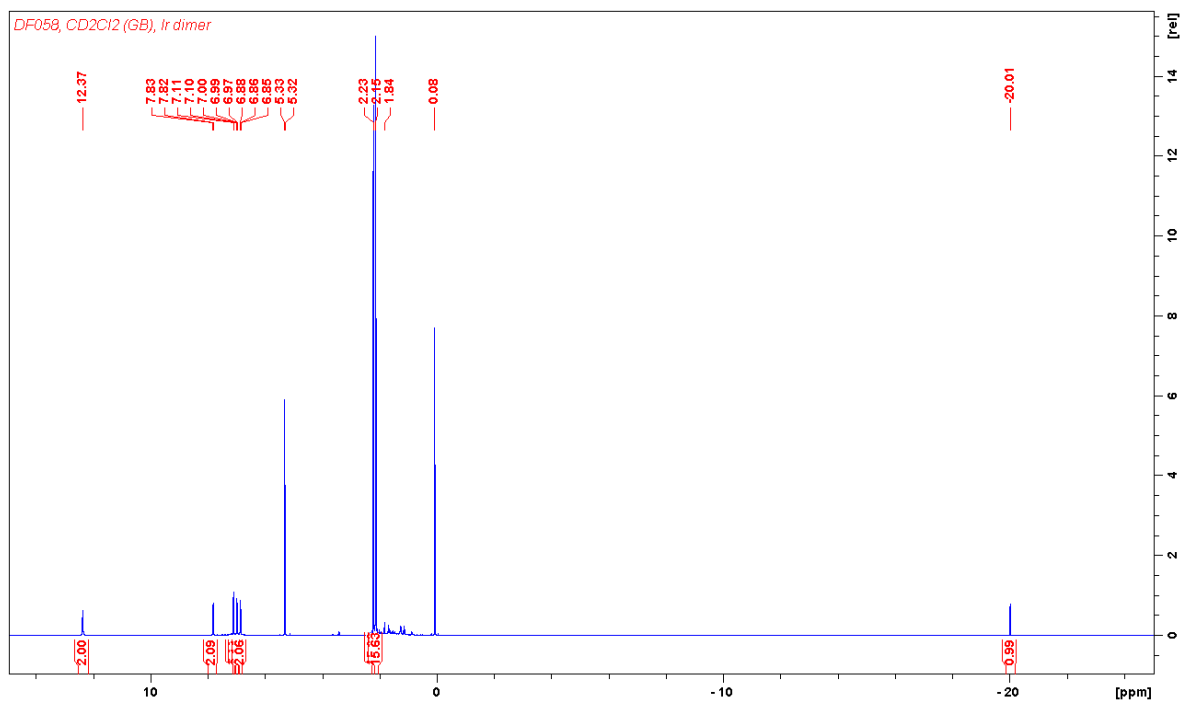


Figure S27. ^1H -NMR (500.23 MHz, CDCl_3) of complex **9**.

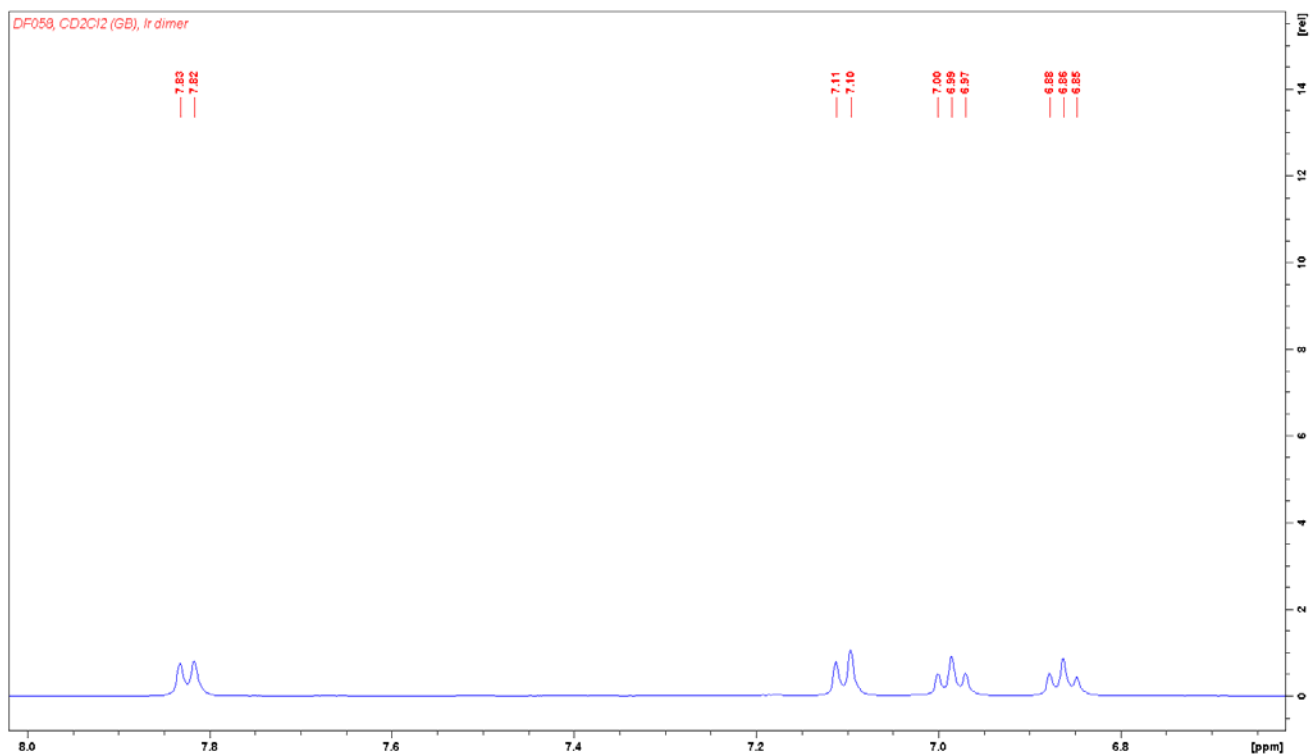


Figure S28. Aromatic region ^1H -NMR (500.23 MHz, CDCl_3) of complex **9**.

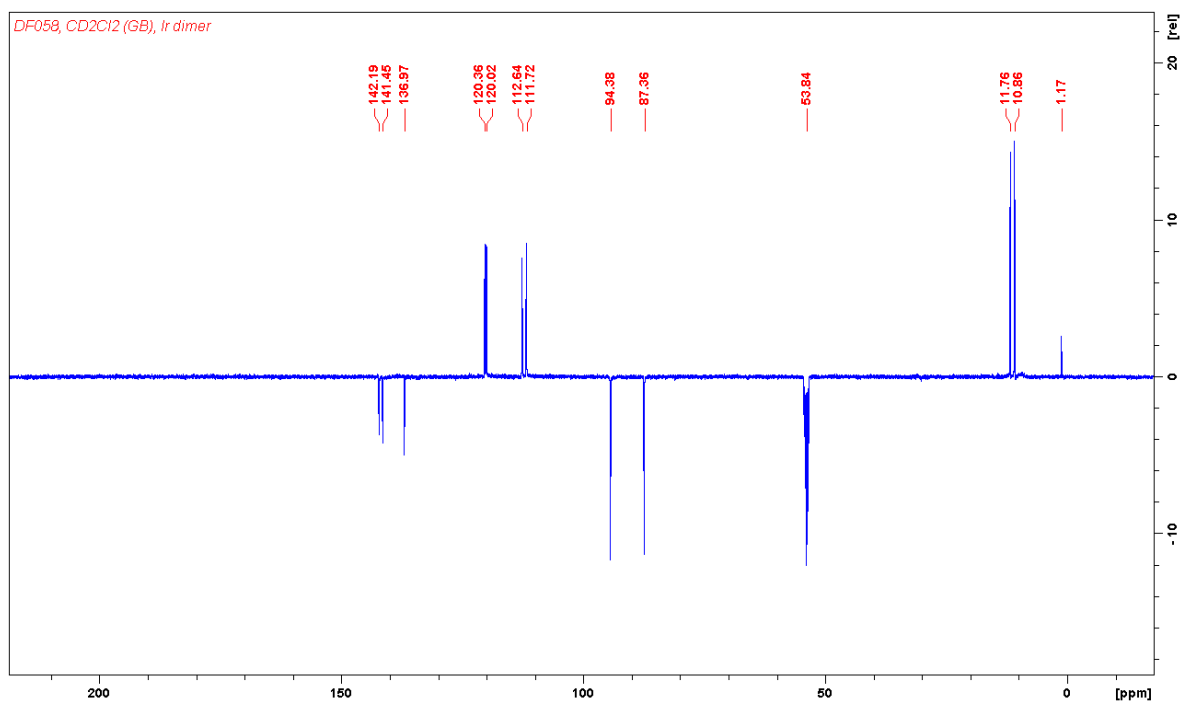


Figure S29. $^{13}\text{C}\{^1\text{H}\}$ -NMR (125.78 MHz, CDCl_3) of complex **9**.

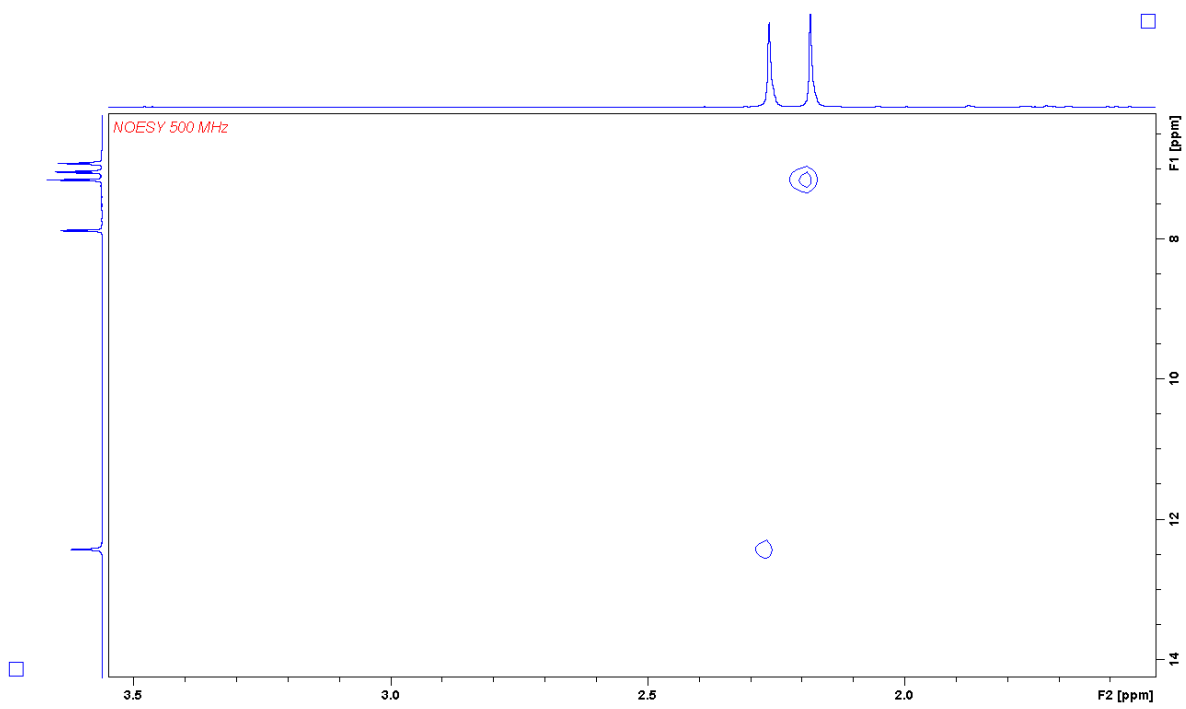


Figure S30. Detail with Cp*-NH correlations in NOESY (500.23 MHz, CDCl₃) of complex **9**.

3. Crystal structure determinations

The single-crystal X-ray diffraction studies of **3**, **4** and **6** were carried out on a Bruker-Nonius at 123(2) K using Mo-K α radiation ($\lambda = 0.71073$ Å). Direct Methods or heavy atom methods (SHELXS-97)⁸ were used for structure solution and refinement was carried out using SHELXL-2013 (full-matrix least-squares on F^2).⁹ Hydrogen atoms were localized by difference electron density determination and refined using a riding model (H(N) free). Semi-empirical absorption corrections were applied. For **3** an extinction correction was applied.

3: red crystals, C₁₇H₁₉I₂IrN₄ · CH₂Cl₂, $M_r = 810.29$, crystal size 0.30 × 0.15 × 0.12 mm, monoclinic, space group $P2_1/n$ (No. 14), $a = 9.463(1)$ Å, $b = 11.757(1)$ Å, $c = 20.717(2)$ Å, $\beta = 95.26(1)^\circ$, $V = 2295.2(4)$ Å³, $Z = 4$, $\rho = 2.345$ Mg/m³, $\mu(\text{Mo-K}\alpha) = 8.75$ mm⁻¹, $F(000) = 1496$, $2\theta_{\text{max}} = 55.0^\circ$, 48478 reflections, of which 5259 were independent ($R_{\text{int}} = 0.025$), 250 parameters, $R_1 = 0.015$ (for 5061 I > 2 σ (I)), $wR_2 = 0.032$ (all data), $S = 1.19$, largest diff. peak / hole = 0.52 / -0.59 e Å⁻³.

4: orange crystals, C₁₇H₂₁I₂IrN₂, $M_r = 699.36$, crystal size 0.30 × 0.10 × 0.06 mm, monoclinic, space group $P2_1/c$ (No. 14), $a = 9.703(1)$ Å, $b = 11.875(1)$ Å, $c = 16.439(2)$ Å, $\beta = 90.10(1)^\circ$, $V = 1894.2(3)$ Å³, $Z = 4$, $\rho = 2.452$ Mg/m³, $\mu(\text{Mo-K}\alpha) = 10.31$ mm⁻¹, $F(000) = 1280$, $2\theta_{\text{max}} = 55.0^\circ$, 24003 reflections, of which 4339 were independent ($R_{\text{int}} = 0.052$), 210 parameters, 2 restraints, $R_1 = 0.025$ (for 3812 I > 2 σ (I)), $wR_2 = 0.062$ (all data), $S = 1.07$, largest diff. peak / hole = 1.47 / -1.77 e Å⁻³.

6: red crystals, C₁₉H₂₅I₂IrN₂, $M_r = 727.41$, crystal size 0.40 × 0.20 × 0.03 mm, orthorhombic, space group $Pbca$ (No. 61), $a = 8.6423(6)$ Å, $b = 17.5203(17)$ Å, $c = 27.4808(18)$ Å, $V = 4161.0(6)$ Å³, $Z = 8$, $\rho = 2.322$ Mg/m³, $\mu(\text{Mo-K}\alpha) = 9.39$ mm⁻¹, $F(000) = 2688$, $2\theta_{\text{max}} = 55.0^\circ$, 44349 reflections, of which 4776 were independent ($R_{\text{int}} = 0.040$), 224 parameters, $R_1 = 0.023$ (for 4295 I > 2 σ (I)), $wR_2 = 0.054$ (all data), $S = 1.08$, largest diff. peak / hole = 1.98 / -1.16 e Å⁻³.

The single-crystal X-ray diffraction study of **9** was performed on a Bruker Kappa ApexII diffractometer with sealed tube and Triumph monochromator ($\lambda = 0.71073$ Å) at a temperature of 150(2) K up to a resolution of $(\sin \lambda/\theta)_{\text{max}} = 0.61$ Å⁻¹. The Eval15 software¹⁰ was used for the intensity integration. For the prediction of reflection profiles a rather large isotropic mosaicity of 1.0 ° was used. A numerical absorption correction and scaling was performed with SADABS¹¹ (correction range 0.51-0.85). A total of 24638 reflections was measured, 13828 reflections were unique ($R_{\text{int}} = 0.028$) leading to an overall completeness of 94.4%. 10816 reflections were observed [$I > 2\sigma(I)$]. The structure was solved with Patterson superposition methods using SHELXT.¹² Structure refinement was performed with SHELXL-2018⁹ on F^2 of all reflections. Two of the four independent solvent molecules were refined with disorder models. In these disorder components, three C atoms were refined isotropically. All other non-hydrogen atoms were refined freely with anisotropic displacement parameters. The hydrogen atoms were introduced in calculated positions. The Ir-H hydrogen atoms were kept fixed at the calculated position. All other hydrogen atoms were refined with a riding model. 918 Parameters were refined with 202 restraints (concerning distances, angles and displacement parameters in the CH₂Cl₂ solvent). R_1/wR_2 [$I > 2\sigma(I)$]: 0.0370 / 0.0906. R_1/wR_2 [all refl.]: 0.0549 / 0.0983. $S = 1.022$. Residual electron density between -2.27 and 1.83 e/Å³. Geometry calculations and checking for higher symmetry was performed with the PLATON program.¹³

9: [C₃₄H₄₁Ir₂N₄]Cl · 2 CH₂Cl₂, $F_w = 1095.41$, red needle, 0.58 × 0.11 × 0.04 mm³, triclinic, $P\bar{1}$ (no. 2), $a = 10.0193(6)$, $b = 19.0273(8)$, $c = 21.4413(11)$ Å, $\alpha = 75.059(2)$, $\beta = 86.963(2)$, $\gamma = 85.500(3)^\circ$, $V = 3935.0(3)$ Å³, $Z = 4$, $D_x = 1.849$ g/cm³, $\mu = 7.13$ mm⁻¹.

CCDC 1915713 (**3**), 1915714 (**4**), 1915715 (**6**) and 1921152 (**9**) contain the supplementary crystallographic data for this paper. These data can be obtained free of charge from The Cambridge Crystallographic Data Centre via www.ccdc.cam.ac.uk/data_request/cif.

⁸ G. M. Sheldrick, *Acta Crystallogr.*, **2008**, *A64*, 112-122.

⁹ G. M. Sheldrick, *Acta Crystallogr.*, **2015**, *C71*, 3-8.

¹⁰ A. M. M. Schreurs, X. Xian, L. M. J. Kroon-Batenburg, *J. Appl. Cryst.*, **2010**, *43*, 70-82.

¹¹ G. M. Sheldrick, **2014**. SADABS. Universität Göttingen, Germany.

¹² G. M. Sheldrick, *Acta Crystallogr.*, **2015**, *A71*, 3-8.

¹³ A. L. Spek, *Acta Crystallogr.*, **2009**, *D65*, 148-155.

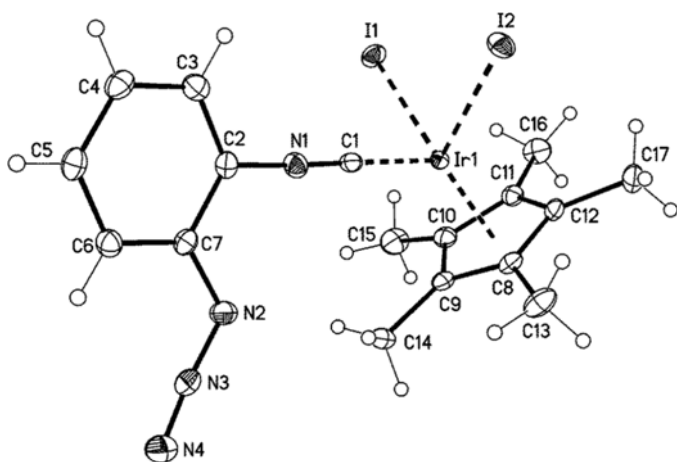


Figure S31. Molecular structure of **3** (solvent omitted for clarity, displacement parameters are drawn at 50% probability level)

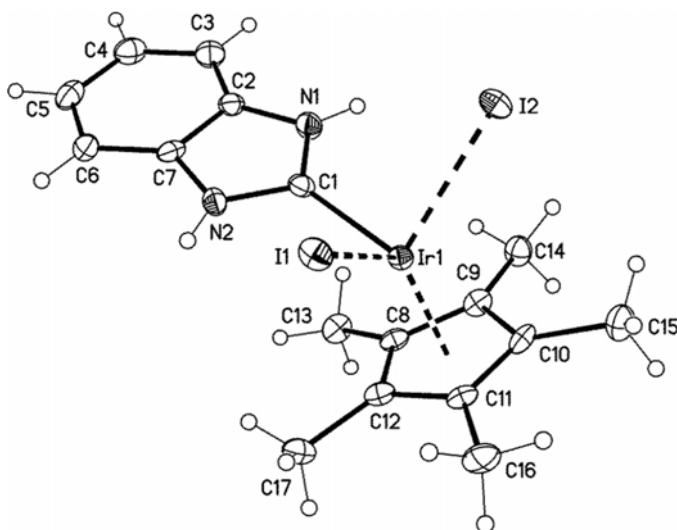


Figure S32. Molecular structure of **4** (displacement parameters are drawn at 50% probability level)

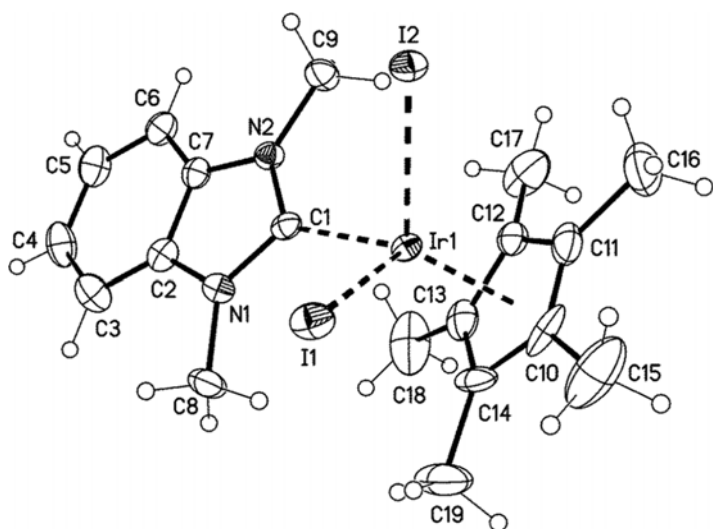


Figure S33. Molecular structure of **6** (displacement parameters are drawn at 50% probability level)

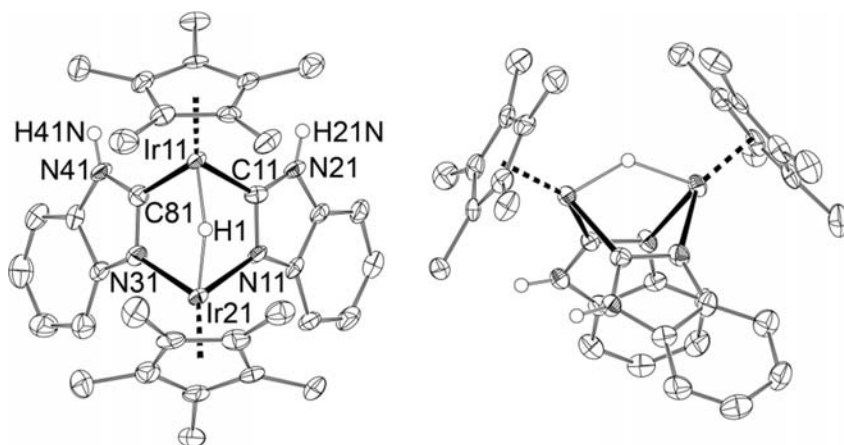


Figure S34. Molecular structure of **9** (only one of two independent molecules is shown. Displacement parameters are drawn at 50% probability level).

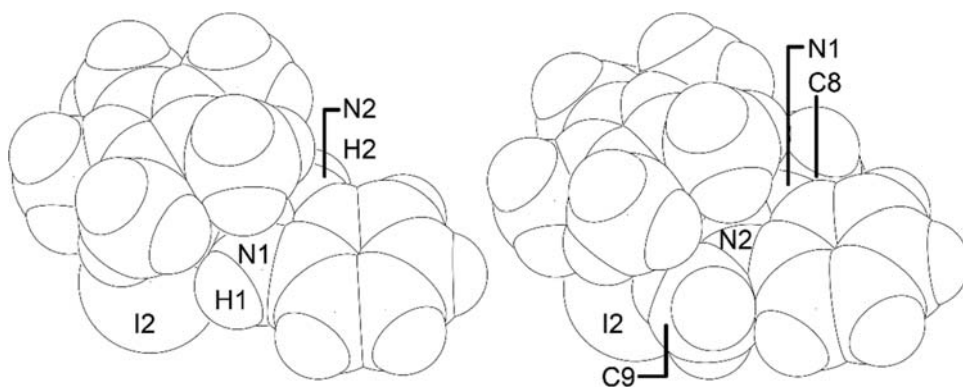


Figure S35. Space-filling (CPK) plots of complexes **4** (left) and **6** (right) in orientations identical to Figure 4.

4. DFT calculations

Computational Procedures

Density functional calculations were performed at the BP86/ZORA/Grimme-D3/TZ2P level of theory¹⁴ using Amsterdam Density Functional (ADF)¹⁵ 2013.01 (geometry optimizations, QTAIM¹⁶) and 2016.102 (ETS-NOCV¹⁷). The nature of each stationary point was confirmed by frequency calculations.

Iridium-carbene bond analysis (ETS-NOCV)

Table S1. ETS-NOCV results (BP86/ZORA/Grimme-D3/TZ2P; kcal mol⁻¹).

	4	4 	6
ΔE_{total}	-67.8	-68.2	-62.7
ΔE_{Pauli}	335.2	316.5	317.8
ΔE_{elstat}	-271.7	-256.5	-255.2
ΔE_{orb}	-131.4	-128.1	-125.3
σ	-90.6	-86.5	-82.6
π_1	-16.6	-17.2	-15.4
π_2	-6.9	-6.7	-8.2
polaris.	-9.4	-9.2	-9.0

¹⁴ a) E. van Lenthe, E.J. Baerends, *J. Comput. Chem.*, **2003**, *24*, 1142–1156. b) E. van Lenthe, E.J. Baerends, J.G. Snijders, *J. Chem. Phys.*, **1993**, *99*, 4597–4610. c) E. van Lenthe, E.J. Baerends, J.G. Snijders, *J. Chem. Phys.*, **1994**, *101*, 9783–9792. d) E. van Lenthe, A. Ehlers, E.J. Baerends, *J. Chem. Phys.*, **1999**, *110*, 8943–8953.

¹⁵ a) G. te Velde, F.M. Bickelhaupt, S.J.A. van Gisbergen, C. Fonseca Guerra, E.J. Baerends, J.G. Snijders, T. Ziegler, *J. Comput. Chem.*, **2009**, *22*, 931–967. b) C. Fonseca Guerra, J.G. Snijders, G. te Velde, E.J. Baerends, *Theor. Chem. Acc.*, **1998**, *99*, 391–403. c) ADF2010/2013/2016, SCM, Theoretical Chemistry, Vrije Universiteit, Amsterdam, The Netherlands, <http://www.scm.com>.

¹⁶ a) R.F.W. Bader, *Atoms In Molecules*, Clarendon Press, Oxford, **1994**. b) J.I. Rodríguez, R.F.W. Bader, P.W. Ayers, C. Michel, A.W. Götz, C. Bo, *Chem. Phys. Lett.*, **2009**, *472*, 149–152. c) J.I. Rodríguez, *J. Comput. Chem.*, **2013**, *34*, 681–686.

¹⁷ M.P. Mitoraj, A. Michalak, T. Ziegler, *J. Chem. Theory Comput.*, **2009**, *5*, 962–975.

Dinuclear complex – QTAIM analysis

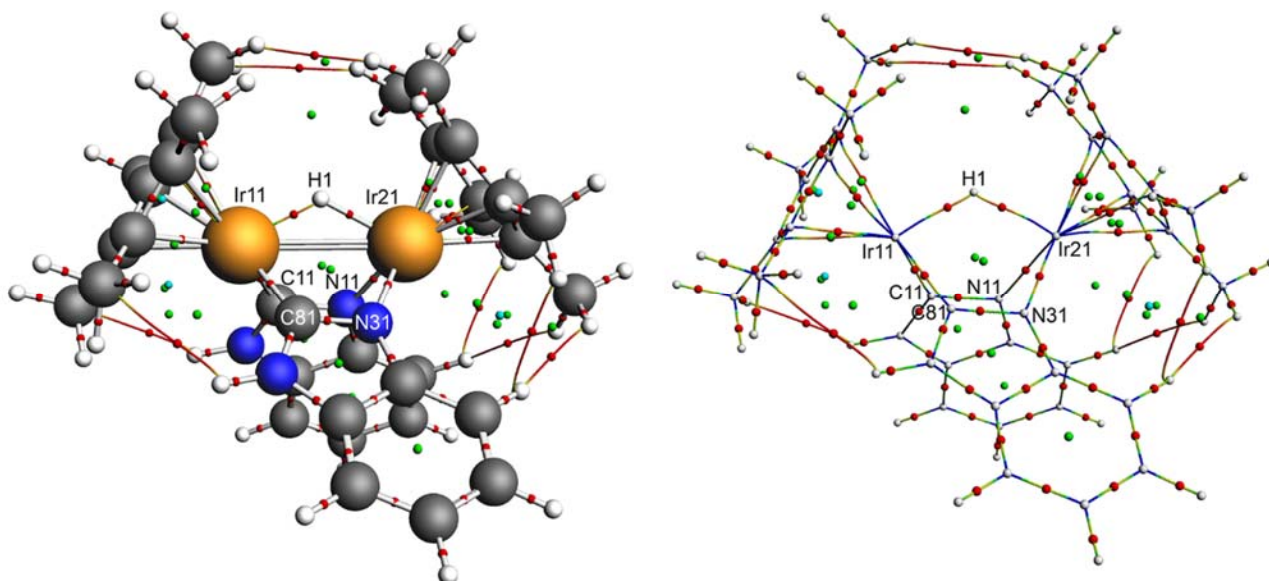


Figure S36. AIM analysis of bond paths in complex 9. Bond critical points in red, ring critical points in green, cage critical points in blue.

Ir21-H1:

CP # 150

(RANK,SIGNATURE): (3,-1)

CP COORDINATES: 0.113662 -0.190354 -1.283076

EIGENVALUES OF HESSIAN MATRIX:

-0.1266267E+00 -0.1176255E+00 0.3703199E+00

EIGENVECTORS (ORTHONORMAL) OF HESSIAN MATRIX (COLUMNS):

0.8894264E+00 -0.1517288E+00 -0.4311601E+00

0.4569990E+00 0.3127751E+00 0.8326606E+00

-0.8517573E-02 0.9376301E+00 -0.3475303E+00

VALUES OF SOME FUNCTIONS AT CP(a.u.):

Rho = 0.9650692E-01

|GRAD(Rho)| = 0.6368909E-15

GRAD(Rho)x = 0.2631921E-15

GRAD(Rho)y = -0.5744514E-15

GRAD(Rho)z = -0.7978459E-16

Laplacian = 0.1260677E+00

(-1/4)Del**2(Rho) = -0.3151691E-01

HESSIAN MATRIX:

-0.3403763E-01 -0.1788360E+00 0.7318250E-01

0.2187987E+00 -0.1411640E+00

-0.5869340E-01

lr11-H1:

CP # 164

(RANK,SIGNATURE): (3,-1)

CP COORDINATES: -0.357104 0.727128 -1.255170

EIGENVALUES OF HESSIAN MATRIX:

-0.1646005E+00 -0.1516453E+00 0.4353025E+00

EIGENVECTORS (ORTHONORMAL) OF HESSIAN MATRIX (COLUMNS):

-0.8838717E+00 0.2358074E+00 0.4039377E+00
-0.4666449E+00 -0.3857964E+00 -0.7958666E+00
0.3183355E-01 0.8919395E+00 -0.4510328E+00

VALUES OF SOME FUNCTIONS AT CP(a.u.):

Rho = 0.1160140E+00
|GRAD(Rho)| = 0.1631405E-14
GRAD(Rho)x = 0.5493714E-15
GRAD(Rho)y = -0.1253037E-14
GRAD(Rho)z = -0.8885787E-15
Laplacian = 0.1190567E+00
(-1/4)Del**2(Rho) = -0.2976417E-01

HESSIAN MATRIX:

-0.6599658E-01 -0.1940357E+00 -0.1065710E+00
0.2173085E+00 0.2108844E+00
-0.3225524E-01

lr11-H1-lr21-N31-C81:

CP # 120

(RANK,SIGNATURE): (3,+1)

CP COORDINATES: 0.387311 0.400059 -0.299717

EIGENVALUES OF HESSIAN MATRIX:

-0.1888460E-01 0.5562107E-01 0.6427222E-01

EIGENVECTORS (ORTHONORMAL) OF HESSIAN MATRIX (COLUMNS):

-0.6544136E+00 -0.7415170E+00 -0.1479708E+00
-0.3165416E+00 0.9094018E-01 0.9442094E+00
0.6866908E+00 -0.6647424E+00 0.2942335E+00

VALUES OF SOME FUNCTIONS AT CP(a.u.):

Rho = 0.3057751E-01
|GRAD(Rho)| = 0.6053094E-16
GRAD(Rho)x = 0.2653959E-18
GRAD(Rho)y = -0.5651706E-16
GRAD(Rho)z = -0.2167363E-16
Laplacian = 0.1010087E+00
(-1/4)Del**2(Rho) = -0.2525217E-01

HESSIAN MATRIX:

0.2390290E-01 -0.1664249E-01 0.3310469E-01
0.5586848E-01 0.1859846E-01
0.2123731E-01

Ir11-H1-Ir21-N11-C11:

CP # 90

(RANK,SIGNATURE): (3,+1)

CP COORDINATES: -0.508760 -0.058241 -0.290503

EIGENVALUES OF HESSIAN MATRIX:

-0.1888377E-01 0.5538984E-01 0.6452279E-01

EIGENVECTORS (ORTHONORMAL) OF HESSIAN MATRIX (COLUMNS):

0.6523083E+00 -0.3388319E+00 -0.6780021E+00
0.3440975E+00 -0.6646404E+00 0.6632119E+00
0.6753449E+00 0.6659175E+00 0.3169592E+00

VALUES OF SOME FUNCTIONS AT CP(a.u.):

Rho = 0.3054789E-01
|GRAD(Rho)| = 0.2719184E-13
GRAD(Rho)x = 0.2353707E-13
GRAD(Rho)y = -0.2062493E-15
GRAD(Rho)z = 0.1361469E-13
Laplacian = 0.1010289E+00
(-1/4)Del**2(Rho) = -0.2525721E-01

HESSIAN MATRIX:

0.2798426E-01 -0.2077800E-01 -0.3468265E-01
0.5061274E-01 -0.1534019E-01
0.2243185E-01
